Dissertation zur Erlangung des Doktorgrades

der Fakultät für Chemie und Pharmazie

der Ludwig-Maximilians-Universität München

Transferrin receptor targeted gene delivery

Şurhan Göl Öztürk

aus

İskilip, Türkiye

2022

Erklärung

Diese Dissertation wurde im Sinne von § 7 der Promotionsordnung vom 28. November 2011 von Herrn Prof. Dr. Ernst Wagner betreut.

Eidesstattliche Versicherung

Diese Dissertation wurde eigenständig und ohne unerlaubte Hilfe erarbeitet.

München, 27.07.2022

.....

Şurhan Göl Öztürk

Dissertation eingereicht am: 01.08.2022

1. Gutachter: Prof. Dr. Ernst Wagner

2. Gutachter: Prof. Dr. Stefan Zahler

Mündliche Prüfung am: 06.09.2022

To My Family

Aileme

Table of Contents

1. Introduction

This chapter should give a brief introduction into the concept of non-viral carriers for nucleic acid delivery to put the experimental data of the thesis into a broader context. It is not a complete review of the whole gene therapy area.

1.1 Nucleic Acid Delivery: Opportunities and Challenges of Non-viral Gene Therapy

After elucidating the molecular structure of nucleic acids [1-3], discovering their role in the coding, transfer and translation of genetic information [4-6] has revolutionized the nucleic acid biology. With the discovery of the genes that cause or relate to diseases, scientists have created a new field for correction of these diseases [7, 8]. Nucleic acid and gene therapy has enormous promise for broad spectrum of clinical applications such as correcting genetic defects and treating infinite diseases [9-12]. However, scientists have made incomparably small progress with these diseases because of very simple but important three problems: “Delivery, delivery and delivery” [13]. There are 3579 studies that reported at the first quarter of 2022 [14], although, the first nucleic acid therapy treatment approved by Food and Drug Administration (FDA) in 1998 (Vitravene®) [15], and first gene therapy treatment approved by European Commission (alipogene tiparvovec, Glybera®) in 2012 [16].

Nucleic acids such as plasmid DNA (pDNA), messenger RNA (mRNA) and small interfering RNA (siRNA) have widely used in nucleic acid and gene therapy studies. Due to the large size, negative charge and biodegradability of naked nucleic acids, they need an appropriate carrier system for the efficient and

specific intracellular delivery. The literature survey of gene therapy will show two main strategies: viral and non-viral delivery systems. In principle, both systems have same aim for efficient uptake and genetic information expression. Unfortunately, there is no ideal gene delivery system each has its own advantages and challenges.

Viruses are sophisticated biological machines with a natural purpose to transport nucleic acids into cells. Viral vectors dominate current clinical gene therapy studies [17]. Despite carrying limited amount of genetic information, viruses can effectively enter the host cell and facilitate their replication. Most of the virus based gene therapy applications take advantage of the viral infection pathway. In general, genes related to viral replication and toxicity are eliminated and this deletion of viral genes can provide available room for desired genetic materials. Viral particles have ability productively infect a specific cell (cellular tropism), tissue (tissue tropism) or host species (host tropism). This feature can prevent nonspecific and/or inefficient uptake of viral particles. Although recent studies have made it possible to generate targeted virus particles, it is very difficult to prevent nonspecific uptake by other cells [18-21]. On the other hand, despite their domination on clinical treatment because of their high efficiency, viral vectors have serious handicaps, such as limited size and cargo type [22], as well as possibility of causing cancer [23] and immunogenicity [24].

Non-viral vectors have made progress in recent times and showed several advantages such as simplicity of use, production of large-scale, biocompatibility, and low immune response. However, they have still need to overcome many limitations. Direct gene transfer with naked pDNA is the simplest non-viral gene

delivery method which is discovered by Wolff and colleagues [25]. The pDNA was directly injected into skeletal muscle and triggered immune response in mouse. This work introduced a new class of therapeutic modalities called 'DNA vaccines' [26]. Subsequently, to increase naked DNA gene transfer efficiency, several approaches have been developed such as gene gun [27] and electroporation [28] which allow DNA directly into the cell even into the nucleus while avoiding enzymatic degradation. However, these physical transfection methods are far from applicable for classical treatment. Therefore, the lipidic, peptide or polymer-based carriers capable of forming particles with therapeutic nucleic acids by electrostatic interaction provide more benefit for non-viral delivery. Nonetheless, the efficiency of synthetic vehicles is still lower than natural carrier viral particles.

1.2 Carrier Requirements

As mentioned section 1.1, both viral and non-viral particles have been studied to carry nucleic acid to create excellent carriers; still they have to handle a lot of challenging tasks. Figure 1 shows in schematic form of critical requirements for nucleic acid journey with carriers. The first and fundament step of a successful nucleic acid therapy is to transfer of the cargos such as pDNA, siRNA or microRNA to the place where it will be active. Therefore, these macromolecules have to protected against degradation in the blood stream until taken up by the target cells [29]. Uptake into the cell usually mediated through endocytic vesicles. Release of nucleic acids into the cytosol or transfer to nucleus (in case of pDNA) is an important step for successful delivery otherwise, they will be degraded in lysosomes [30, 31]. In this journey, the carriers should act like multitasking shuttles. Carriers need to be consistently associated with their cargo in the

extracellular environment. When the time is right, they must properly dissociate from their cargo for functionality inside the cell.

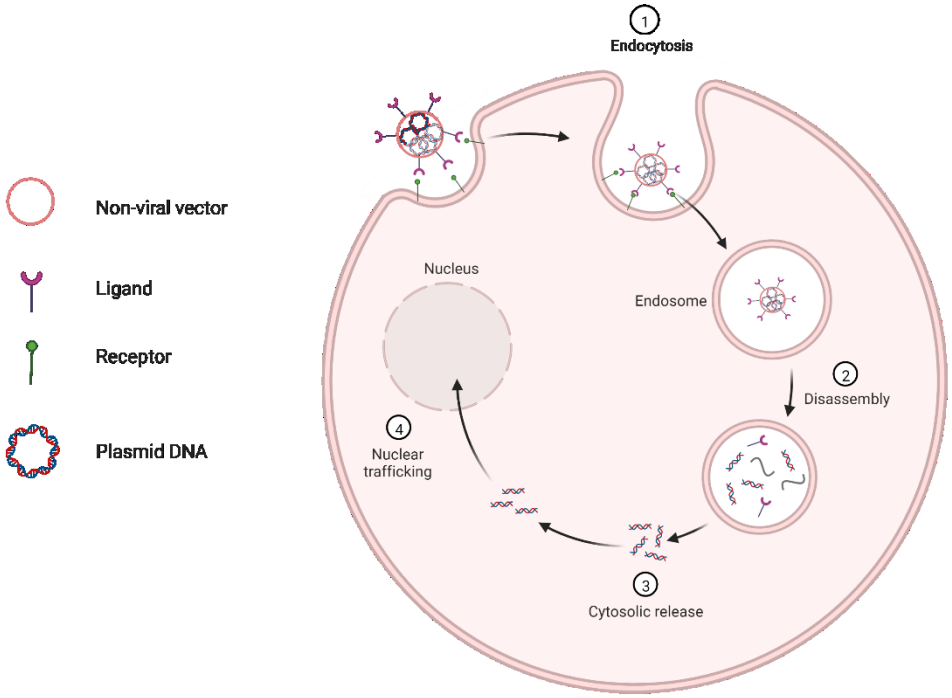

Figure 1 Targeted non-viral transfection of the cell. Adapted from “Cancer Cell-Targeted Gene Therapy”, by BioRender.com (2022). Retrieved from https://app.biorender.com/biorender-templates.

Different extracellular or intracellular sites have unique microenvironment properties. Carriers can be designed according to these environmental differences to get through the successful delivery process [32]. React to changes in enzyme activities, pH or the redox can be beneficial for carrier design. Bioreducible elements are important tools because of their redox potential that differs greatly in the extracellular and intracellular regions [33].

1.2.1 Nucleic Acid Complexation

It is useful to create complexed and condensed form with particles to prevent the rapid clearance of free DNA from the blood stream. This compacted form of DNA provides protection against nucleases and increases the circulation time. The ionic interaction between negatively charged nucleic acids and multivalent cations is a frequently and conveniently used mechanism for nucleic acid complexation. This interactions form nanosize complexes called ‘polyplexes’ [34, 35]. However, the interaction can be considered successful as long as it can escape the endosome when the time comes.

The size of nanoparticles has crucial role on the pharmacokinetics and biodistribution. While particles below a certain size (5.5 nm) are cleared from the kidney quickly, up to 400 nm sized particles accumulate in solid tumors as a result of enhanced permeability and retention (EPR) effect [36, 37]. Even so, type of cancer determines the extent of passive accumulation and the limit of size that can pass through tumor vessels [38, 39]. Other important issues are destabilization of the polyplex caused by interaction with proteins and electrolytes in the biological fluids and dissociation with nucleic acid due to counter ion exchange in the cell. Stability of particles depends on size and charge, however this can be enhanced with additional tools such as crosslinking or hydrophobic elements [40-43].

Non-viral carriers generated by solid-phase synthesis (SPS) can be composed of only natural amino acids, only artificial building blocks or a combination of both. Previously some homopolymers were used, such as lysine, ornithine and arginine, which have the ability to bind and condense with nucleic acids [44-47].

Afterwards, defined oligopeptides began to be used which are produced by SPS [48-51]. SPS provide an opportunity to design and produce variety of structures to select suitable artificial vectors for further optimization. Thus, most suitable, nontoxic particles can be selected among many options for nucleic acid compaction, extracellular stability, transfection efficiency, endosomal escape and nucleic acid release in cytosol [52, 53].

Lipid nanoparticles (LNPs) are advanced non-viral vectors that are used for delivery of various nucleic acids and drugs. They have sphere shape, nanosize and one or more ionizable lipids in their structure. Due to the positive charge of these lipids, negative charged nucleic acids can compose internal aqueous phase of the LNPs [54-56]. LNPs can manage cargo release in late endosome (pH 5.5-6.5) with use cationizable lipids [57]. These cationizable lipids are not cytotoxic with their natural charge at physiological pH [58].

1.2.2 Vector Shielding

Nucleic acid complexation usually results in formation of nanoparticles with positive surface potential. These cationic carriers can improve the transfection efficiency *in vitro* by binding with negatively charged cell surface and/or provide endosomal escape [59, 60], however their nonspecific uptake and interaction with cells and blood components is not desirable. The polyethylene glycol (PEG) leads the way as most common and well established shielding agent which can increase the circulation time of nanoparticles [61] and has been successfully used including SPS-designed nanocarriers [62-64]. Apart from PEG, there are many other alternative hydrophilic agents (Figure 2) that are used in nucleic acid delivery such as hydroxyethyl starch (HES) [65], poly(N-(2-hydroxypropyl)

methacrylamide) (pHPMA) [66], repeats of Pro-Ala-Ser (PAS) [67] and polysarcosine [68].

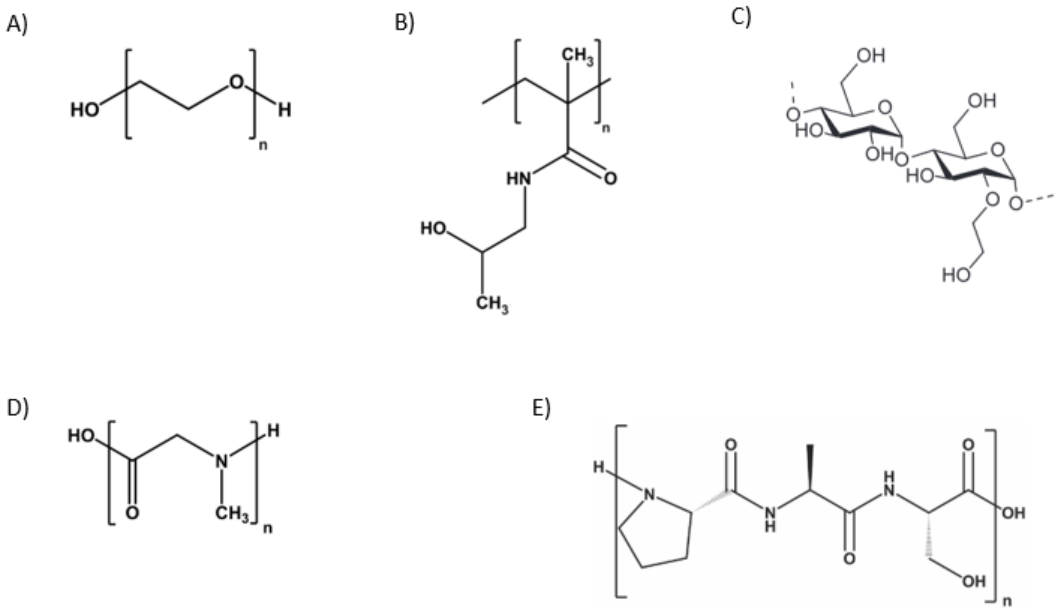

Figure 2 Chemical structure of agents used for shielding. A) Polyethylene glycol (PEG), B) poly(N-(2-hydroxypropyl) methacrylamide) (pHPMA), C) hydroxyethyl starch (HES), D) polysarcosine, E) repeats of Pro-Ala-Ser (PAS).

The PEG molecules may have some safety concerns like formation of anti-PEG antibodies [69] and negative effect of nucleic acid complexation [70]. The polyplex size and stability are affected by the length of PEG chain and ratio of hydrophilic polymer to cationic polymer in the polyplex [71, 72]. Pre- or post-addition of the PEG to the nanocarriers are also effective in nucleic acid compaction. For example, post-PEGylation can improve nucleic acid compaction [73, 74].

Contrarily, Üzgün and colleagues showed pre-PEGylation was improved mRNA binding and transfection [59].

PEGylation brings with it the “PEG dilemma” which is increase of nanoparticle stabilization and circulation time versus decrease cellular uptake and endosomal escape [75]. Therefore, PEG alternatives or pH triggered cleavage of PEGs in endosome [76] can overcome this dilemma.

1.2.3 Targeting for Delivery of Genetic Information

Plasma membrane by its lipophilic and negatively charged structure is the main barrier that prevents transport of large and charged molecules. Use of electrostatic interactions between cell membrane and produced particles can enhance cellular internalization. However, this adsorptive endocytosis cannot be as specific and effective as receptor mediated uptake [77]. Therefore, attachment of targeting ligands to the carriers is convenient approach to increase effective and specific cellular internalization. An appropriate ligand which can be proteins, peptides, glycoproteins and antibodies is generally selected from overproduced receptors in cancer cells or target cells [78].

The group of Ruoslahti identified arginine–glycine–aspartic acid (RGD) [79], which is specific integrin binding motif that frequently used peptide in nucleic acid delivery [80-83]. In a recent published study, polycondensed peptide carriers modified with a cyclic RGD showed up to a 2-3 fold decrease in proliferative activity for pDNA suicide gene therapy [84].

Asialoglycoprotein receptor (ASGPR) is a membrane protein which is highly expressed by parenchymal hepatocytes [85]. One of the recent research showed

that their ASGPR targeted nanocarriers are able to successfully bind, protect against proteases and deliver the pDNA *in vitro* [86].

The epidermal growth factor receptor (EGFR) has been targeted by multiple ligands because of its overexpression in different tumor cells. The first approach of pDNA delivery to EGFR expressing cells was with monoclonal anti-EGFR modified polyplexes [87]. Later on, natural epidermal growth factor (EGF) containing carriers showed that number of ligand on the carrier effects not only particle size but also uptake [88]. As a short alternative of EGF peptide, GE11 identified [89]. Xu et al. demonstrated that docetaxel (DTX) and siRNA loaded, GE11 peptides conjugated liposomes enhanced anti-tumor and apoptotic effects against cancer cells [90].

The folate receptor (FR) is a 38 kDa [91] membrane glycoprotein that overexpressed on tumor cells to transport folate/folic acid (FA) [92]. FR is widely used in different vectors such as oligomers [93] or lipo-oligomers [94] and with different cargos such as pDNA [95] or siRNA [96]. Formerly, uptake of FR targeted poly-L-lysine (PLL) based DNA polyplexes were used for receptor mediated delivery and showed 6 fold higher transfection than nontargeted polyplexes [97]. However, excess of free ligand can block or compete with the targeted polyplexes for the receptor mediated endocytosis. Leamon et al. showed that receptor mediated uptake depends to ligand concentration and spatial distance with polyplexes [98]. FR targeted delivery has mainly studied with siRNA. FA decorated siRNA nanocarriers have demonstrated higher gene silencing both *in vitro* and *in vivo* [96, 99, 100]. Moreover, FA polyplexes highly accumulated in tumor tissue rather than other tissues [101] and its cellular toxicity

is lower than non-FA polyplexes [96]. Interestingly, FA conjugation provided decreased zeta potential and increased blood circulation.

Another commonly used ligand for targeted gene delivery studies is transferrin (Tf). As the Tf receptor is the main focus of the thesis, this ligand will be explained in detail at section 1.3.

Combination of more than one targeting ligands can enhance transfection efficiency which is termed as dual targeting. Kos et al. showed that combination of B6 and GE11 ligands had most efficient pDNA delivery with DU145 prostate cancer cell culture which has both receptors [102]. In recently published study, HA and anti-HER2 antibody were used together and clear synergetic effect observed in siRNA delivery. Dual targeted nanoparticles could not be accessed by degradative enzymes because of densely condensed structure of the complex that results in increased biostability [103].

1.2.4 Endosomal Escape

In previous section, the journey of nanoparticles is presented until their uptake by cells. Nanoparticles have significant potential to protect cargo, cell or tissue specific targeted delivery and cargo release within a desired cellular region. The most important step of delivery is cellular internalization through endocytotic pathway [104, 105]. This mechanism comprises several steps: (1) uptake into endocytic vesicle, (2) form into the early endosomal compartment, (3) maturation into late endosome, and finally (4) accumulation in the lysosome [106]. The pH of endosomes decreases step by step from physiological pH 7.4 to ~pH 6.5 in the early, ~pH 6.0 in the late endosome and ~pH 5.0 in the lysosome [107]. Major

roles of these vesicles are sorting, trafficking and recycling of endocytosed material. Most challenging part of the delivery is to escape from endocytic pathway without degradation.

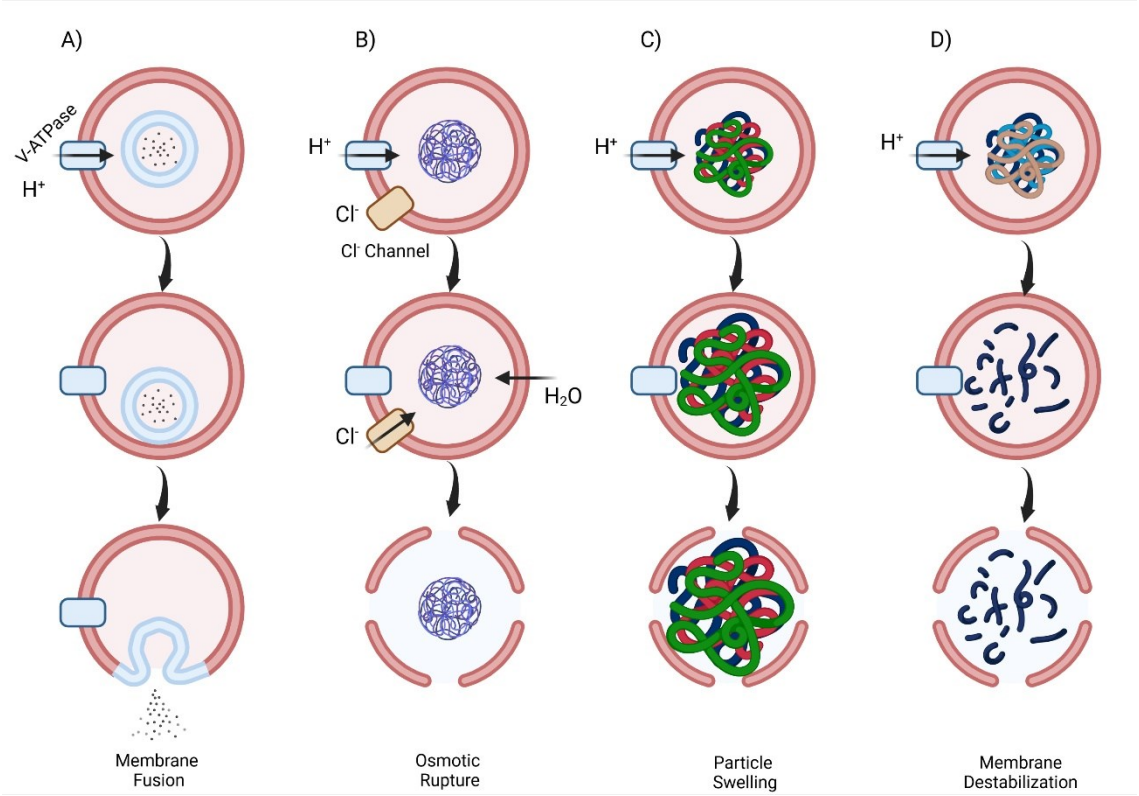

Figure 3 Schematic representations of the proposed mechanisms of endosomal escape. Adapted from Smith et al. [105]. Created with BioRender.com.

Some viruses and liposomes use lipidic cell membrane fusion to succeed escaping from the endosome (Figure 3A). Additionally, this mechanism can be used by hybrid lipid polymers which combine polymer core and lipid shells. For

instance, hierarchically nanoassembled arginine functionalized gold nanoparticles were developed to transport protein into the cytosol. Encapsulated proteins were released into the cytosol immediately after nanoparticle contact with the endosome membrane [108].

Another endosomal escape mechanisms is the proton sponge effect that described by Jean-Paul Behr to explain endosomal escape of nanocarriers with buffering capacity [109]. In this mechanism, decrease of pH in the endosome is inhibited by polymer with buffering capacity and cause continuation of proton pumping to reach the desired pH. Due to buffering of the endosomal pH, active transport of protons is triggered by V-ATPases which causes the passive diffusion of chloride counterions. This results in increase of osmotic pressure with water flow into the vesicle and finally osmotic rupture (Figure 3B). The transfection agent polyethylenimine (PEI) exhibits endosomal escape performance [110], but also cytotoxicity [111, 112]. Later on, oligoaminoethylene building blocks with even numbered amine groups showed highest buffer capacity and enhanced transgene expression *in vitro* and *in vivo* [95].

One of the other proposed endosomal escape concept is the swelling of the pH responsive nanoparticles (Figure 3C). The pH-sensitive PDEAEMA-core/PAEMA-shell nanoparticle showed swelling from ~200 to 550 nm with decreased pH from 7.4 to 4.9. These increased sized particles released calcein and protein ovalbumin into the DC2.4 dendritic cells [113].

Polymer nanoparticles can be designed for membrane destabilization to enhance endosomal escape (Figure 3D). However, there are several limitations during endosomal escape via membrane destabilization such as decreased cellular

viability, timing of the destabilization and the size of loaded therapeutic. To minimize the cytotoxicity, polyplexes from poly(aspartamide) derivatives were developed. They showed membrane destabilization at pH 5.5 but minimal damage at pH 7.4 and high pDNA transfection efficacy without cellular toxicity [114]. Whereas small molecules can be released from endosome, relatively bigger particles can be trapped during membrane destabilization. The poly(β-amino ester) nanoparticles stabilized by a PEG lipid could chaperone 3 or 10 kDa dextran but not 40 and 70 kDa [115].

1.2.5 Intracellular and Nuclear Trafficking

The fate of cargo highly dependent on the carrier, cell type, intracellular routes, cargo type and size [116-118]. As mention in section 1.2.4, bottleneck of delivery process is endosomal release even with effective nanoparticles. Cellular compartment of action differs depending on type of nucleic acid cargo. Whereas siRNA and mRNA only need to reach the cytoplasm to mediate function, pDNA needs to enter nucleus thorough cytoplasm for transcription (Figure 1). In the typical *in vitro* transfection, 36 % of polyplexes can traffic via endosome and 1 % of pDNA can reach nucleus. However, only 0.01 % of pDNA can enter inside the nucleus and there is 50 % chance for transgene expression [119].

Nuclear membrane is the next barrier of the nucleic acid delivery and nuclear import is size dependent process [120]. Only small molecules can pass through the nuclear pore complex (NPC). Therefore, bigger particles need to wait for cell division to be inside of the nucleus. Unfortunately, cell division is not an option for non-dividing cells. Branched PEI showed increased transfection efficiency in the G2/M phase, conversely, there was no cell cycle dependency with linear PEI

[121]. Conjugation of nuclear localization signal (NLS) peptides might be a solution to avoid cell cycle dependency for DNA transfection [122]. However, mechanism of NLS peptides has not been clearly elucidated.

1.3 Transferrin Receptor Targeted Nucleic Acid Delivery

As mention in previous sections, gene and nucleic acid therapy are exciting alternative for cancer treatments. Due to the many side effect of irradiation, surgery and chemotherapy, classical treatments are not comfortable for patients and reduce their quality of life. Therefore, both viral and non-viral nanocarriers have been exploded because of their specificity and ability to modify cargo and nanocarrier structure. However, for effective nucleic acid delivery, there are several challenges to overcome such as protection of cargo, cell/tumor specific uptake, efficient endosomal escape and finally release of cargo in active form in the proper cell compartment. Several nucleic acid nanocarriers have been developed such as “polyplexes” and “LNPs” which were specifically investigated in this thesis.

The receptor mediated endocytosis increases the specific uptake of therapeutic nucleic acids into tumor cells. The transferrin receptor (TfR, CD71) is a favorable candidate for targeting due to its low level of expression in normal human cells and overexpression in most tumor cells [123, 124]. The human Tf receptor (hTfR) has two identical 95 kDa subunits and is responsible for the majority of cellular iron uptake into cells [125]. Iron has important role on DNA synthesis, cell division, and cellular metabolism which is taken into the cells through TfR mediated endocytosis. The Tf has molecular weight of 80 kDa with 679 amino acid residues [126, 127]. Plasma Tf can be found in different forms regarding to

its iron binding such as apo-Tf (noniron bound), monoferric or diferric (holo-Tf) forms [128].

Tf is one of the most studied targeting ligand due to its nonimmunogenicty and availability from human with relatively low cost. However, use of a large serum derived Tf protein have difficulties in pharmaceutical work because of suitable protein source and protein stability. Therefore, same receptor targeted but smaller synthetic ligands would be preferable. The 12 amino acid length TfR targeting peptide (H-THRPPMWSPVWP-NH_2) binds the TfR at different region from natural Tf ligand avoiding competition and causes receptor mediated endocytosis [129]. Nevertheless, this peptide rapidly is degraded by serum proteases in 30 min half-life. Thus, protease resistant TfR ligands developed that containing all amino acids in *D*-configuration and reverse sequence (retro-enantio TfR (reTfR): H-pwvpswmpprht-NH_2) [130]. This protease resistance synthetic peptide has capacity to transport of cargo across the blood brain barrier (BBB) which is one of the most restrictive barrier in the human body. Additionally, owing to slow clearance from blood circulation, reTfR highly accumulated in the mice brains without toxicity. Section 3.1 “Transferrin Receptor Targeted Polyplexes” part of the thesis focuses on reTfR as a targeting ligand.

Transferrin targeted nucleic acid delivery has displayed promising clinical potential with pDNA [131-133] and siRNA [134]. The Tf modified PLL based polyplexes increased gene delivery compared nonmodified polyplexes via receptor mediated endocytosis without any cell toxicity [135]. Tf decorated cationic PEI polymer was also used as a next generation polyplexes to enhance gene delivery [63, 136-139]. Another delivery system with Tf is novel

oligoaminoamides (OAAs) based delivery which have lower molecular weight than amino ethylene based delivery and still contains nucleic complexation and endosomal buffer capacity [140, 141]. Zhang et al. showed 100 fold increase gene transfection with Tf-PEG-OAA polyplexes compared nonmodified polyplexes [142]. In following study, they also achieved 80 % gene silencing and tumor growth reduction with Tf modified PEG-OAAs [143].

The LNPs also have great potential for therapeutic nucleic acid delivery. Most famous example of LNPs are mRNA based vaccines that used in the COVID-19 pandemic [144-146]. Rapid development and use of this system against COVID-19 pandemic was also due to long-term study focusing on development of patient specific cancer vaccination based on the patient specific tumor RNA transcriptome [147-150]. Surface modifications of LNPs are also possible which can improve circulation time, promote targeting, enhance cargo transfection and avoid particle aggregation. For instance, Tf conjugated LNPs that produced by single-step microfluidic synthesis showed enhanced therapeutic effect both *in vitro* and *in vivo* [151]. In another study, Tf modified PEI-based lipid nanoparticles used to deliver antisense oligo LOR-2501. Tf modified nanoparticles showed high transfection *in vitro* with low toxicity in HepG2 cells as well [152]. Section 3.2 “Transferrin Receptor Targeted LNPs” part of the thesis investigates hTf as a targeting ligand for modified LNPs.

1.4 Aim of the Thesis

The therapeutic nucleic acids have promising potential with many clinical applications however, there are still few authorized examples in the market. Despite reaching encouraging clinical effects, there are many challenges to overcome such as design and production of safe and efficient non-viral delivery systems. Even though production, formulation and storage of plasmid DNA vectors are easier than other nucleic acid therapeutics, entering the cell nucleus is fundamental necessity for encoded gene expression. Additionally, nucleic acid vectors need carriers to protect them during their journey from nucleic acid complexation, cellular uptake, endosomal escape to intracellular cargo release at the target site. Non-viral vectors mostly deliver their cargo to cells without any specificity that cause undesired side effects. Specificity of cellular uptake can be achieved by decoration of nanocarriers with ligands. Transferrin receptor is frequently used in targeted gene delivery. The thesis focuses on the transferrin targeted pDNA delivery using two different nanocarriers: lipo-oligoaminoamides (lipo-OAAs) with small synthetic peptide reTfR and lipid nanoparticles (LNPs) with natural human transferrin ligand.

The first aim of thesis was to incorporate a small synthetic reTfR ligand as targeting module into pDNA polyplexes that are based on precise, sequence-defined components. For this purpose, previously developed T-shaped lipo-OOAs compacted with pDNA (pCMV-Luc) were to be used. Evaluation of the efficiency and comparison of the physicochemical and transfection characteristics were to be compared between two main groups: nonmodified and reTfR modified polyplexes. Properties such as size, zeta potential, morphology,

stability, transfection efficiency and especially cellular association of the polyplexes had to be investigated.

The second aim of the thesis was to explore LNPs for transferrin targeted pDNA delivery. For this purpose, pDNA LNPs with different PEG ratios were to be evaluated with different amount of hTf ligands to precise optimum transfection efficiency. Size, zeta potential, morphology, stability, transfection efficiency and cellular association of the polyplexes were to be investigated *in vitro*.

2. Material and Methods

2.1 Materials

The materials used for the experiments are presented in Table 1.

Table 1 Materials used for experimental procedures

Materials	CAS-No./Cat-No.	Supplier
1 kDa dialysis membrane	1966.1	Carl Roth (Karlsruhe, Germany)
4′,6-diamidino-2-phenylindole (DAPI)	D9542	Sigma-Aldrich (Munich, Germany)
Agarose NEEO Ultra	9012-36-6	Carl Roth (Karlsruhe, Germany)
Antibiotics	P4333	Sigma-Aldrich (Munich, Germany)
CellTiter-Glo®	G7571/2/3	Promega (Mannheim, Germany)
Cholesterol	C8667	Sigma-Aldrich (Munich, Germany)
Cy5-labeling kit	MIR3700	Mirus Bio LLC (Madision, WI, USA)
D-(+)-Glucose monohydrate	14431-43-7	Merck Millipore (Darmstadt, Germany)
D-Lin-MC3-DMA	1224606-06-7	Hycultec (Beutelsbach, Deutschland)
Beetle luciferin sodium salt	E1605	Promega (Mannheim, Germany)
DMEM	D6046	Sigma-Aldrich (Munich, Germany)
DMG-PEG2000	160743-62-4	Avanti Polar Lipids (Alabama, USA)
DOPE	4004-05-1	Avanti Polar Lipids (Alabama, USA)
DSPE-PEG-N_3	1938081-40-3	Avanti Polar Lipids (Alabama, USA)
Ethidium bromide (EtBr)	E1510	Sigma-Aldrich (Munich, Germany)
Fetal bovine serum (FBS)	F9665	Sigma-Aldrich (Munich, Germany)
Flasks and multi-well plates	-	TPP (Trasadingen, Switzerland)
GelRed	41003	VWR International GmbH (Darmstadt, Germany)
HEPES	7365-45-9	Biomol (Hamburg, Germany)

Human transferrin	11096-37-0	Sigma-Aldrich (Munich, Germany)
Ligands	-	Teoman Benli-Hoppe (LMU Pharmaceutical Biotechnology)
LPEI	9002-98-6	In-house synthesis [153]
Luciferase cell culture lysis buffer	E1500	Promega (Mannheim, Germany)
pCMVLuc	PF461	PlasmidFactory (Bielefeld, Germany)
RPMI-1640	R2405	Sigma-Aldrich (Munich, Germany)
Sequence-defined oligomers	-	Simone Berger [154], Lun Peng (LMU Pharmaceutical Biotechnology)
Trypsin-EDTA	P10-024 100	PAN-Biotech (Aidenbach, Germany)

The buffers used for the experiments are presented in Table 2.

Table 2 Buffers used for experimental procedures

Buffer	Composition
Citrate buffer	10 mM Citric acid, pH 4.0
Electrophoresis loading buffer	6 ml glycerine, 1.2 ml 0.5 M EDTA solution (pH 8.0), 2.8 ml H_2O, 20 mg bromophenol blue
FACs buffer	10 % FBS in PBS
HBG	20 mM HEPES, 5 % glucose, pH 7.4
HEPES	20 mM HEPES, pH 7.4
LAR Buffer	20 mM glycylglycine, 1 mM $MgCl_2$, 0.1 mM EDTA, 3.29 mM DTT, 0.548 mM ATP (adenosine 5′-triphosphate), 0.55 mM Coenzyme A stock solution, pH 8.0-8.5
Luciferin	10 mM Luciferin-Na, 1M Glycylclycine, pH 8.0,
Phosphate-buffered saline (PBS)	137 mM NaCl, 2.7 mM KCl, 8.1 mM Na_2HPO_4,1.5 mM KH_2PO_4, pH 7.3-7.5
TBE buffer	89 mM Trizma® base, 89 mM boric acid, 2 mM EDTA-Na_2, pH 8.0

2.2 Methods

The following sections contain methods for transferrin receptor targeted polyplexes and transferrin receptor targeted LNPs. Methods of transferrin receptor targeted polyplexes have been adapted from:

Benli-Hoppe T,[+] **Göl Öztürk Ş**,[+] Öztürk Ö, Berger S, Wagner E, Yazdi M. Transferrin Receptor Targeted Polyplexes Completely Comprised of Sequence-Defined Components, Macromol Rapid Commun. 2021 Oct 29:e2100602.

[+] Equally contributing first authors

2.2.1 Synthesis of Oligomers and Ligands

All oligomers (lipo-OAAs) were synthesized by Simone Berger or Lun Peng (LMU Pharmaceutical Biotechnology). The synthesis of lipo-OAAs is explained in previous studies [154, 155]. All ligands were synthesized by Teoman Benli-Hoppe (LMU Pharmaceutical Biotechnology) and explained in our recently published study [156]. All lipo-OAAs and ligands were synthesized by SPS and will be explained by Simone Berger, Lun Peng and Teoman Benli-Hoppe in their theses.

2.2.2 Formation and Biophysical Characterization of pDNA Nanoparticles

2.2.2.1 Polyplex Formation

The plasmid pCMVLuc pDNA and lipo-OAAs at an indicated molar nitrogen/phosphate ratio (N/P) of 12 were separately diluted in equal volume of 20 mM HEPES buffer with 5 % glucose (HBG buffer, pH 7.4). The N/P ratio was calculated under consideration of only protonatable nitrogens. Then nucleic acid

and lipo-OAA solutions were rapidly mixed by pipetting (10 times) and incubated 30 min for pDNA formulations at room temperature (RT). For post functionalization, 0.5 equivalent (equiv) of dibenzocyclooctyne (DBCO) agent per azido-lipo-OAA were added to polyplex solution. This mixture was rapidly mixed at least 5 times by pipetting and incubated for 4 h at RT. For comparison, the same procedures were also performed with unmodified polyplexes, but HBG was added instead of modifying DBCO agents.

2.2.2.2 LNP Formation

For all following LNP studies, pDNA was also used as nucleic acid cargo. The LNP formulations were prepared based on the protocol developed by Franziska Haase (LMU Pharmaceutical Biotechnology) via mixing one volume of lipids and oligomers in ethanol. An N/P ratio of 9 for ionizable lipooligomer CLO3 (Lun Peng, LMU Pharmaceutical Biotechnology) and 4.5 for D-Lin-MC3-DMA (MC3) were used. Cholesterol, 1,2-dioleoyl-sn-glycero-3-phosphorylethanolamine (DOPE), 1,2-dimyristoyl-rac-glycero-3-methoxypolyethylene glycol-2000 (DMG-PEG) and MC3 were mixed at 48:20:2:30 mole ratios for MC3 formulation. Cholesterol, DOPE, DMG-PEG, 1,2-distearoyl-sn-glycero-3-phosphoethanolamine-N-[α-azido(polyethylene glycol)-2000] (ammonium salt) (DSPE-PEG-N_3) and CLO3 at 45:20:**2**:**3**:30 (2:3) or 45:20:**1**:**4**:30 (1:4) mole ratios for LNP with CLO3 oligomer formulation. Three volumes of pDNA (200 ng/well) containing citrate buffer solutions (pH 4.0) were mixed with one volume lipid mixture and incubated for 10 min at RT. The resulting LNPs were dialyzed against HEPES for 2 h to remove the ethanol and restore the pH to neutral. After dialyses, LNP formulations were post functionalized with 1, 2 or 3 equiv of DBCO agent per DSPE-PEG-N_3 were

added to LNP solution and mixed at least 5 times by pipetting and incubated for 4 h at RT. The 1.25 µl of 10 mM iron (III) citrate buffer (200 mM citrate, pH 7.8) per milligram of Tf content was added for iron incorporation into hTf [63]. The same procedures were also performed with unmodified LNPs, but HEPES was added instead of modifying agents.

2.2.2.3 Particle Size and Zeta Potential

Particle size, zeta potential and polydispersity index (PDI) were characterized by dynamic and electrophoretic light scattering (DLS, ELS) and measured in a folded capillary cell (DTS1070) by Zetasizer Nano ZS with backscatter detection (Malvern Instruments, Worcestershire, Germany). Nonmodified and modified (0.5 equiv of DBCO agents) pDNA polyplexes were prepared with final pDNA concentration of 1 µg pDNA in a total volume of 125 µl HBG. After size measurement, the pDNA samples were diluted to 800 µl with HBG and zeta potential measurement was done. For size (z-average) and PDI measurements, the equilibration time was 0 min, the temperature was 25 °C, refractive index was 1.330 and the viscosity was 0.8872 mPa•s. For the zeta potential measurements 15 sub runs at 25°C were chosen. The Smoluchowski equation was used for calculation of zeta potential. LNP formulations prepared as described above (Section 2.2.2.2). LNPs (200 ng pDNA) in total volume of 80 µl were mixed with total of 800 µl HEPES. For measurement of particle size, zeta potential and PDI, same protocol was used. All samples were measured in triplicate.

2.2.2.4 Agarose Gel Shift Assay for pDNA Binding

A 1 % agarose gel for pDNA was prepared with TBE buffer (trizma base 10.8 g, boric acid 5.5 g, disodium EDTA 0.75 g and 1 L of water). After boiling and cooling down to about 50 °C, GelRed (Biotium, Inc., Hayward, CA, USA) was added and the solution was casted in the electrophoresis unit. Polyplexes (200 ng of pDNA in 20 µl HBG) and LNPs (200 ng of pDNA in 20 µl HEPES) were prepared and then mixed with 4 µl loading buffer (6 ml of glycerin, 1.2 ml of 0.5 M EDTA, 2.8 ml of H_2O, 0.02 g of bromophenol blue). All samples were transferred into the gel pockets and electrophoresis was performed at 120 V for 80 min in TBE buffer.

2.2.2.5 Ethidium Bromide Exclusion Assay

pDNA polyplexes (2 µg pDNA, 200 µl) were formed at N/P 12 as described above (Section 2.2.2.1) and optionally modified with 0.5 equiv of PEG-1. HBG was used as blank and the 100 % value determined by free pDNA (2 µg in 200 µl HBG). EtBr solution (700 µl, 0.5 µg/ml) was added to each sample solutions and incubated for 3 min. The fluorescence intensity of EtBr was measured using a Cary Eclipse Fluorescence Spectrophotometer (Varian, now part of Agilent Technologies, Germany). The excitation wavelength was set to λ_{ex} = 510 nm, and the emission wavelength to λ_{em} = 590 nm. The data is presented as fluorescence intensity of EtBr in relation to free pDNA.

2.2.2.6 Particle Imaging by Transmission Electron Microscopy (TEM)

Polyplexes were prepared as described in section 2.2.2.1 for polyplexes but in water instead of HBG and in section 2.2.2.2 for LNPs in HEPES. Carbon coated copper grids (Ted Pella, Inc. USA, 300 mesh, 3.0 mm O.D.) were hydrophilized

by argon plasma (420 V, 1 min). They were placed on a 10 µl sample droplet for 3 min. Then the droplet was removed, and the grid was washed with 5 µl of staining solution (1 % uranyl formate in purified water). Immediately afterwards, it was stained for 5 sec with the same solution. The solution was removed, and the grid was allowed to be dried for 20 min. All grids were analyzed with a JEOL JEM-1100 electron microscope (JEOL, Tokyo, Japan) at 80 kV acceleration voltage.

2.2.3 Biological Characterization *in vitro*

2.2.3.1 Cell Culture

The human erythroleukemic suspension cell line K562 (ATCC CCL-243) was cultured in RPMI-1640 medium and the murine adherent neuroblastoma cell line Neuro-2a (N2a, ATCC CCL-131) was cultured in low glucose (1 g/L glucose) Dulbecco's Modified Eagle Medium (DMEM). The cell culture mediums were supplemented with 10 % FBS, 4 mM L-glutamine, 100 U/ml penicillin and 100 µg/ml streptomycin. All cells were cultured at 37°C and 5 % CO_2 in an incubator with a relative humidity of 95 %.

2.2.3.2 Luciferase Gene Transfer

K562 suspension cells were seeded in V-shaped 96-well plates with 3×10^4 cells per well at 2-3 h before pDNA transfection. N2a cells were seeded in 96-well plates 1×10^4 per well at 24 h. Then the medium was replaced with 75 µl of the fresh serum-containing medium right before the transfection. Polyplex solutions (N/P 12, 25 µl HBG containing 200 ng of pCMVLuc) were added to each well. HBG and linear PEI (LPEI) polyplexes (N/P 6) were used as negative and positive

control, respectively. For LNPs, K562 cells again were seeded in V-shaped 96-well plates with 3 × 10^4 cells per well at 2-3 h before pDNA transfection. Then the medium was replaced with 80 µl of the fresh serum-containing medium right before the transfection. LNPs solutions (N/P 9, 20 µl 200 ng of pDNA in HEPES) were added to each well. HEPES and MC3 formulation (N/P 4.5) were used as negative and positive control, respectively. All samples and controls were performed in triplicate. K562 cells were incubated with polyplexes or LNPs for 24 h at 37 °C. N2a cells were incubated for 4 h with polyplexes, then medium was replaced, and the cells were incubated for further 20 h at 37 °C. Read-out (luciferase activity or metabolic activity measurement) was conducted 24 h after transfection.

In the case of luciferase assay, 100 µl of lysis buffer (12.5 mM tris(hydroxymethyl) aminomethane buffer (pH 7.8) with phosphoric acid, 1 mM dithiothreitol (DTT), 2 mM 1,2-diaminocyclohexane-N,N,N',N'-tetraacetic acid, 5 % glycerol, 0.5 % Triton® X-100; Promega, Mannheim, Germany) was added to each well and incubated for 45 min at RT. Luciferase activity was measured with a Centro LB 960 plate reader luminometer (Berthold Technologies, Bad Wildbad, Germany) in 35 µl cell lysate using a LAR buffer solution (20 mM glycylglycine, 1 mM $MgCl_2$, 0.1 mM EDTA, 3.29 mM DTT, 0.548 mM ATP (adenosine 5′-triphosphate), 0.28 mM Coenzyme A stock solution, pH 8.0-8.5) supplemented with 10 % (v/v) mixture of 10 mM luciferin and 29.375 mM glycylglycine.

2.2.3.3 Cellular Association and Competition Assays

K562 suspension cells were seeded in V-shaped 96-well plates with 3 × 10^4 cells per well at 2-3 h before the experiment. N2a cells were seeded in 96-well plate

with 2 × 10^4 cells per well at 24 h before the experiment. Prior to transfection, the medium was replaced with 75 µl of fresh medium per well for 96-well plate and 450 µl for 24-well plate. For treatment, polyplexes were prepared with 200 ng pDNA (in 25 µl HBG including 20 % Cy5 labeled pDNA). HBG was used as negative control. All experiments were performed in triplicate. Cells were incubated with corresponding polyplexes for 45 min at 37 °C in 5 % CO_2 and washed with phosphate-buffered saline (PBS) three times. Adherent cells were detached with trypsin-EDTA, centrifuged and cell pellets were resuspended in FACs buffer (10 % FBS in PBS) for subsequent measurement.

For LNP formulations, K562 suspension cells were seeded in V-shaped 96-well plates with 3 × 10^4 cells per well at 2-3 h before the experiment. Prior to transfection, the medium was replaced with 80 µl of fresh medium per well. For treatment, LNPs were prepared with 200 ng pDNA (in 20 µl HEPES including 20 % Cy5 labeled pDNA). HEPES was used as negative control. All experiments were performed in triplicate. Cells were incubated with LNPs for 45 min at 37 °C in 5 % CO_2 and washed with PBS three times. Cells were resuspended in FACs buffer for subsequent measurement.

For the transferrin blockade experiment, same procedure was done, however, cells were incubated with free iron saturated hTf (5 mg/ml) for 30 min on ice prior to transfection in order to block and deplete the cell surface transferrin receptors. The 1.25 µl of 10 mM iron (III) citrate buffer (200 mM citrate, pH 7.8) per milligram of Tf content was added for iron incorporation into hTf [63].

Cellular association was measured by CytoFLEX S flow cytometer (Beckman Coulter, Brea, CA, USA) through excitation of Cy5 at 635 nm and detection of

emission at 665 nm. Cells were gated based on the forward- and side-scatter profile. Dead cells were detected by 4′,6-diamidino-2-phenylindole fluorescence (DAPI) staining. FlowJo® 7.6.5 flow cytometric analysis software (FlowJo, Ashland, OR, USA) was used for data analysis.

2.2.3.4 Metabolic Activity of Transfected Cells

For the cell viability assay, after 24 h incubation medium was removed and replaced with 25 µl of medium and 25 µl of CellTiter-Glo® Reagent (Promega, Mannheim, Germany) each well. Samples were incubated on an orbital shaker for 30 min at RT and measured with Centro LB 960 plate reader luminometer (Berthold Technologies, Bad Wildbad, Germany). The relative cell viability (in %) was calculated according to HBG treated negative control cells by following formula: $[A]_{test} / [A]_{control} \times 100$.

2.2.4 Statistical Analysis

Statistical analysis of the results (mean ± sd) was evaluated by two-tailed t-test (unpaired) or one-way ANOVA. Significance levels were set as not significant (ns), *$p \leq 0.05$, **$p \leq 0.01$, ***$p \leq 0.001$ and ****$p \leq 0.0001$.

3. Results and Discussion

3.1 Transferrin Receptor Targeted Polyplexes

This chapter has been adapted from:

Benli-Hoppe T,[+] **Göl Öztürk Ş**,[+] Öztürk Ö, Berger S, Wagner E, Yazdi M. Transferrin Receptor Targeted Polyplexes Completely Comprised of Sequence-Defined Components, Macromol Rapid Commun. 2021 Oct 29:e2100602.

[+] Equally contributing first authors

3.1.1 Design and Synthesis of Sequence-Defined Polyplex Core and Shell Components

Different cargos need different nanocarriers for their delivery. All specific cargo needs their nanocarriers to have specific biophysical properties for intracellular compartment delivery [157]. A good condensation into nanoparticles is key for pDNA cargo because of its large size [52, 67]. Therefore, in this thesis six different lipo-OAAs selected (Table 3) for pDNA delivery that have a balance between stability and cargo release for transcription [154]. These six T-shaped lipo-OAAs have different lipidic diacyl side chains that are composed of either decanoic acid (DecA), nonamido octanoic acid (NonOcA), or oleic acid (OleA). The side chains attached to the cationizable OAA backbone via lysine (K). All six lipo-OAAs have an N-terminal azido-lysine, for post functionalization with DBCO agents via click chemistry [155, 158-160]. Lipo-OAAs can be divided according to presence of glycine-disulfide block (G-ssbb) [33] at the branching point or

terminal cysteines (C). As a first step of polyplexes formation, pDNA and lipo-OAAs produce a core complex (Figure 4).

Table 3 Sequence list of the investigated lipo-oligoaminoamides. The ID numbers are database identification numbers. Lipo-OAAs were designed by Simone Berger (LMU Pharmaceutical Biotechnology).

Lipo-OAA ID Number	Sequences (N → C)
1284	H_2N-K(N_3)-Y_3-(H-Stp)$_2$-H-K(G-ssbb-K(DecA)$_2$)-H-(Stp-H)$_2$-Y_3-COOH
1276	H_2N-K(N_3)-C-Y_3-(H-Stp)$_2$-H-K(K(DecA)$_2$)-H-(Stp-H)$_2$-Y_3-C-COOH
1285	H_2N-K(N_3)-Y_3-(H-Stp)$_2$-H-K(G-ssbb-K(NonOcA)$_2$)-H-(Stp-H)$_2$-Y_3-COOH
1258	H_2N-K(N_3)-C-Y_3-(H-Stp)$_2$-H-K(K(NonOcA)$_2$)-H-(Stp-H)$_2$-Y_3-C-COOH
1218	H_2N-K(N_3)-Y_3-(H-Stp)$_2$-H-K(G-ssbb-K(OleA)$_2$)-H-(Stp-H)$_2$-Y_3-COOH
1214	H_2N-K(N_3)-C-Y_3-(H-Stp)$_2$-H-K(K(OleA)$_2$)-H-(Stp-H)$_2$-Y_3-C-COOH

In the second step, the core polyplexes were post functionalized with PEG-conjugated ligand (Figure 4). All shielding and targeting conjugates are listed in Table 4. Ligands and one or two N-terminally attached DBCO groups linked with a monodisperse PEG_{24} spacer as a surface shielding reagent. Click reaction between DBCO in ligands and azide units in lipo-OAAs provide selectivity, high yield and enhanced reaction kinetics [161-164]. The number of DBCO residues in targeting conjugates can affect targeting efficiency [158, 159]. Therefore, one or two DBCO containing ligands and their control were used in this study. Additional succinyl-trioxa-tridecandiamine (STOTDA) were present in the structure for two DBCO units as a short hydrophilic spacer. As a targeting agent, DBCO-PEG_{24} conjugated retro-enantio reTfR [130] were generated with (*D*)-configuration amino acids to avoid protease degradation. The reTfR contains 12

amino acids with reversed sequence from original (*L*)-peptide [129]. The scrambled peptide (scr-reTfR) sequence (vprhptsppmww) were designed as a targeting control reagent. PEG_{24}-DBCO (PEG) was designed as a negative control. Arginine (R)-PEG also synthesized and might provide hydrophilic or electrostatic effect on the polyplexes because of its positive charge. To enhance stability of both reTfR and scr-reTfR peptide ligands against peptidase, amide unit was chosen as end group.

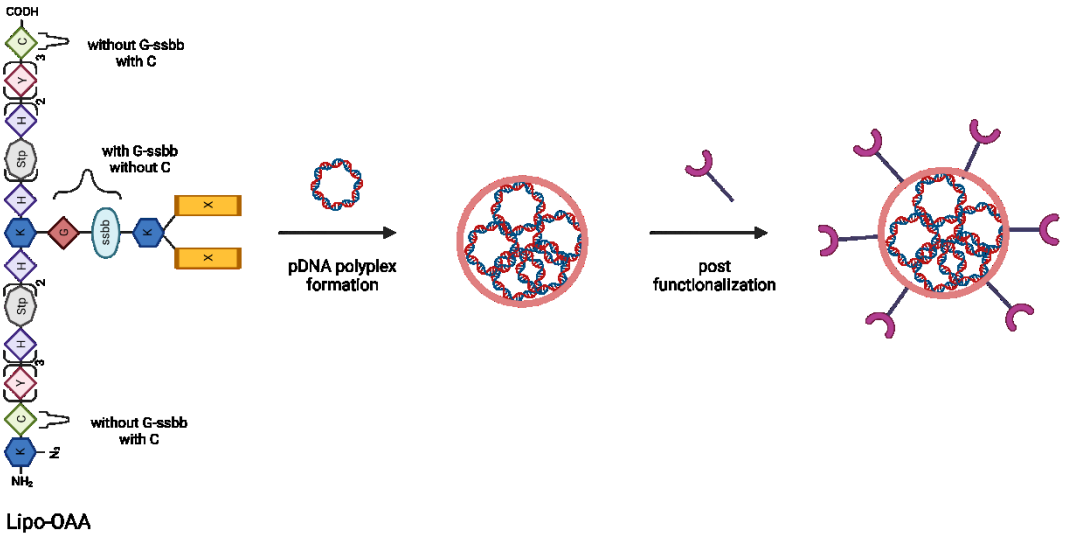

Figure 4 Formation of pDNA lipo-polyplexes in a two-step process. pDNA core lipo-polyplexes were prepared with lipo-OAAs and pDNA, then post functionalizated with mono or bivalent DBCO-PEG_{24}-ligand reagents. Created with BioRender.com.

Table 4 List of the DBCO-PEG_{24}-ligand reagents. Ligands were designed and synthesized by Teoman Benli-Hoppe (LMU Pharmaceutical Biotechnology).

PEG Reagent	Sequence of Ligand (N-C)	End Group
PEG-1, PEG-2		-COOH
reTfR-1, reTfR-2	*pwvpswmpprht-$CONH_2$*	-$CONH_2$
R-PEG-1, R-PEG-2	*R*	-COOH
scr-reTfR-1, scr-reTfR-2	*vprhptsppmww*	-$CONH_2$

3.1.2 Physicochemical Characterization of Functionalized pDNA Polyplexes

For all following studies, plasmid pCMVLuc (encoding *Photinus pyralis* firefly luciferase under control of cytomegalovirus promotor and enhancer) [165] was used as nucleic acid cargo. pDNA core polyplexes were formed in HBG at a previously optimized N/P ratio of 12 using six T-shaped azido lipo-OAAs that were recently designed as part of a larger library screen [154]. These core polyplexes were post functionalized with 0.5 equiv of the different DBCO agents that schematized in Figure 4. Nanoparticle size and zeta potential of pDNA polyplexes were characterized by DLS and ELS (Table 5).

Consistent with the previous study [154], nonmodified pDNA core polyplexes had diameter between 70 and 120 nm with positive zeta potentials between +14 and +32 mV. Their PDIs (Table 5) were low (<0.2), indicating well-formed nanoparticles. reTfR-1 and reTfR-2 modified pDNA polyplexes also displayed low PDIs, sizes between 75 and 95 nm, and only slightly reduced positive surface charge between +12 and +20 mV. The number of DBCO units (mono or bivalent) in the conjugate did not significantly affect their characteristics. With regard to the

control reagents, PEG-1/2 or R-PEG-1/2 modification resulted in polyplexes of similar sizes around 100 nm diameter for most lipo-OAAs. These PEG reagents mediated a clear reduction in zeta potential, ranging for PEG-2 between +2 and +10 mV and for R-PEG-2 between +5 and +8 mV. Polyplexes with scrambled peptide conjugates scr-reTfR-1 and scr-reTfR-2 were in the expected range, with slightly larger sizes (95 to 266 nm) and a lower zeta potential (+10 to +16 mV) than the reTfR polyplexes.

Notably, lipo-OAA 1285 showed comparable polyplex formation without or with reTfR targeting conjugates, but in contrast to the other lipo-OAAs a micrometer-sized aggregate formation with all six control conjugates (scr-reTfR-1/2, PEG-1/2, and R-PEG-1/2). This aggregate formation could not be confirmed via transmission electron microscopy (TEM, see further) and the reasons remain unclear. Lipo-OAA 1285 (like 1258) contains the detergent-like nonamido-octanoic acid (NonOcA) as lipidic domain, which might provide less lipophilic polyplex stabilization. Lipo-OAA 1258 displayed slightly larger polyplex sizes (130 to 266 nm) upon scr-reTfR or R-PEG modification.

Table 5 Particle size (Z-av), zeta potential (Zeta) and PDI of pDNA polyplexes (formed at N/P 12), nonmodified or modified with 0.5 equiv of shielding and targeting agents, were measured by DLS and ELS (mean ± sd, n = 3).

ID	non			reTfR-1			reTfR-2			PEG-1			PEG-2		
	Z-av (nm)	***Zeta (mV)***	***PDI***	***Z-av (nm)***	***Zeta (mV)***	***PDI***	***Z-av (nm)***	***Zeta (mV)***	***PDI***	***Z-av (nm)***	***Zeta (mV)***	***PDI***	***Z-av (nm)***	***Zeta (mV)***	***PDI***
1284	90.6 ± 0.1	13.7 ± 0.4	0.14 ± 0.01	93.3 ± 1.9	15.1 ± 0.2	0.16 ± 0.04	85.8 ± 1.8	16.7 ± 1.5	0.14 ± 0.02	97.8 ± 2.6	7.3 ± 0.4	0.18 ± 0.01	102.4 ± 1.0	3.6 ± 0.2	0.12 ± 0.01
1276	89.6 ± 0.7	32.2 ± 0.9	0.14 ± 0.01	82.6 ± 0.4	20.1 ± 0.8	0.15 ± 0.03	76.7 ± 0.5	17.9 ± 1.5	0.13 ± 0.01	77.7 ± 0.7	13.5 ± 1.1	0.17 ± 0.03	76.7 ± 1.0	10.4 ± 0.5	0.19 ± 0.01
1285	87.8 ± 0.8	16.0 ± 0.3	0.14 ± 0.01	89.0 ± 1.6	19.4 ± 1.0	0.11 ± 0.00	86.4 ± 1.3	17.8 ± 0.7	0.13 ± 0.01	4173 ± 110	-0.5 ± 0.8	0.34 ± 0.12	4811 ± 657	2.3 ± 0.2	0.37 ± 0.04
1258	70.0 ± 0.8	21.8 ± 1.8	0.12 ± 0.02	81.5± 1.1	18.9 ± 1.2	0.13 ± 0.01	75.0 ± 0.5	20.0 ± 0.9	0.13 ± 0.02	78.5 ± 0.3	17.9 ± 1.5	0.21 ± 0.01	72.9 ± 0.3	8.0 ± 0.2	0.16 ± 0.01
1218	119.8 ± 1.7	18.1 ± 0.9	0.19 ± 0.02	87.5 ± 0.2	19.1 ± 1.4	0.11 ± 0.02	89.0 ± 1.4	18.4 ± 1.6	0.10 ± 0.02	80.8 ± 0.8	19.0 ± 1.0	0.21 ± 0.00	87.5 ± 0.3	8.0 ± 0.8	0.16 ± 0.02
1214	104.4 ± 1.3	21.2 ± 0.9	0.15 ± 0.03	91.2 ± 0.6	12.2 ± 1.5	0.13 ± 0.03	83.3 ± 1.0	17.6 ± 1.0	0.12 ± 0.02	82.7 ± 0.3	12.0 ± 1.5	0.12 ± 0.03	85.6 ± 0.5	2.9 ± 0.3	0.12 ± 0.04

ID	scr-reTfR-1			scr-reTfR-2			R-PEG-1			R-PEG-2		
	Z- av (nm)	*Zeta (mV)*	*PDI*	*Z- av (nm)*	*Zeta (mV)*	*PDI*	*Z- av (nm)*	*Zeta (mV)*	*PDI*	*Z- av (nm)*	*Zeta (mV)*	*PDI*
1284	181.4 ± 3.6	10.7 ± 1.1	0.19 ± 0.01	117.7 ± 1.3	14.0 ± 0.8	0.14 ± 0.02	103.3 ± 1.7	8.9 ± 1.1	0.16 ± 0.03	98.7 ± 0.3	6.6 ± 0.9	0.16 ± 0.03
1276	154.0 ± 0.8	11.3 ± 1.2	0.13 ± 0.01	104.3 ± 0.4	13.0 ± 0.6	0.13 ± 0.01	88.3 ± 1.4	9.4 ± 1.2	0.13 ± 0.01	89.0 ± 0.8	5.9 ± 1.4	0.11 ± 0.01
1285	4807 ± 492	11.3 ± 0.5	0.20 ± 0.08	921.4 ± 65	12.5 ± 0.7	0.59 ± 0.06	6012 ± 406	2.2 ± 0.2	0.35 ± 0.18	766.3 ± 23	5.0 ± 0.4	0.59 ± 0.03
1258	265.6 ± 4.1	10.1 ± 0.4	0.24 ± 0.02	128.1 ± 0.6	11.2 ± 1.0	0.17 ± 0.01	131.2 ± 0.8	9.1 ± 0.5	0.14 ± 0.03	90.3 ± 0.6	6.3 ± 1.1	0.15 ± 0.02
1218	108.1 ± 0.6	16.1 ± 2.1	0.11 ± 0.03	128.8 ± 1.8	12.7 ± 2.0	0.25 ± 0.00	97.0 ± 0.5	13.2 ± 1.1	0.09 ± 0.03	96.7 ± 0.4	7.9 ± 1.3	0.09 ± 0.00
1214	95.0 ± 0.4	14.1 ± 0.8	0.10 ± 0.01	98.6 ± 0.0	12.6 ± 1.2	0.14 ± 0.02	93.6 ± 0.4	12.1 ± 0.4	0.09 ± 0.01	92.3 ± 0.6	7.8 ± 0.1	0.11 ± 0.03

TEM measurements showed homogenous and spherical-shaped nanoparticles for all selected pDNA polyplexes in the range of 35 to 50 nm (Figure 5). This apparent discrepancy with DLS results was already previously observed and can be explained by fixation/dehydration for TEM and the high sensitivity of DLS for a minor fraction of aggregates. An agarose gel shift confirmed excellent pDNA binding ability without any pDNA release for all lipo-OAAs polyplexes with or without surface modification (Figure 6), indicating that the chosen OAAs were efficient for successful pDNA binding.

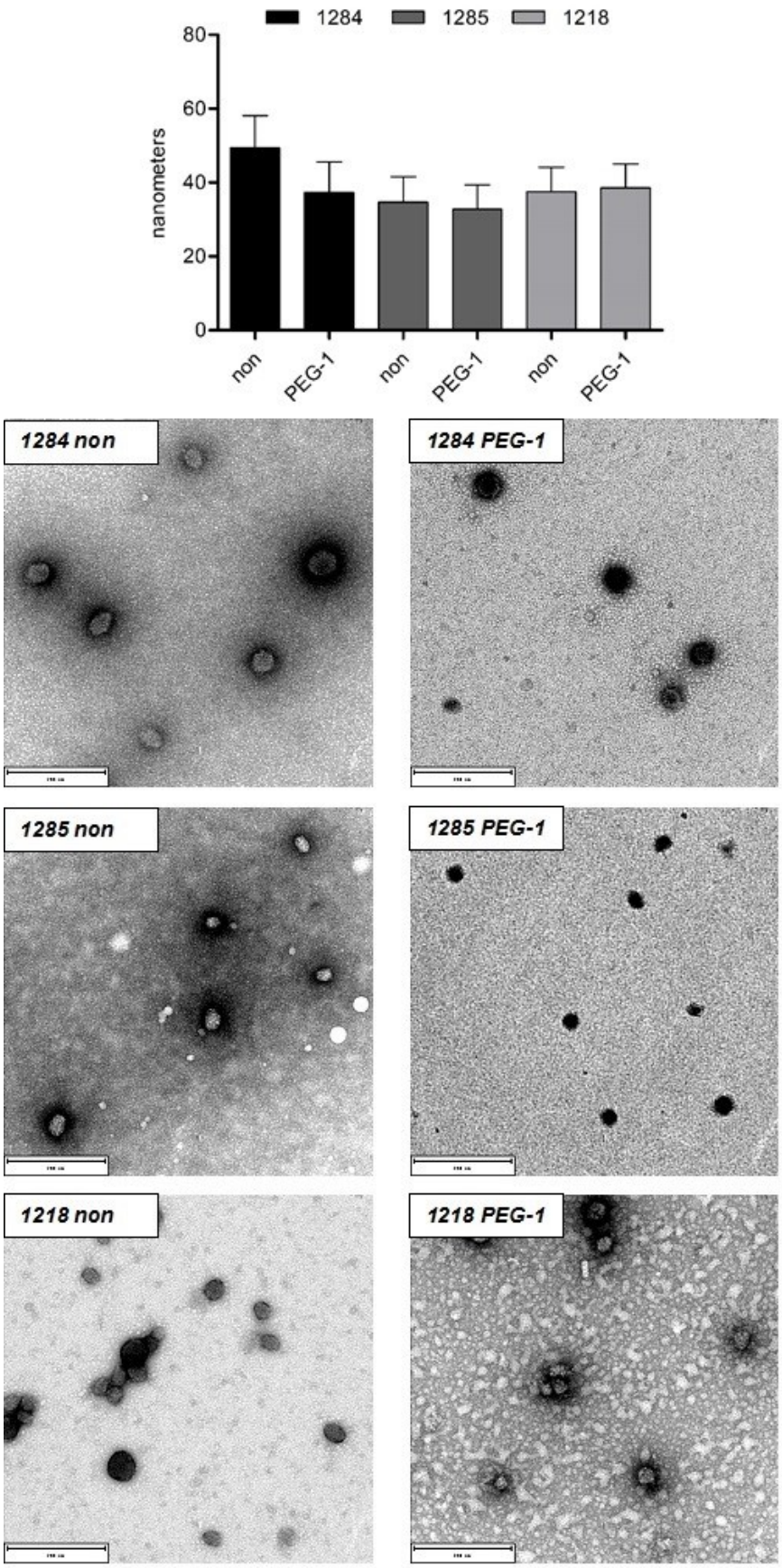
1284
1285
1218
nanometers
80
60
40
20
0
non
PEG-1
non
PEG-1
non
PEG-1
1284 non
1284 PEG-1
1285 non
1285 PEG-1
1218 non
1218 PEG-1

Figure 5 Top: TEM size data (diameter, nm) of pDNA lipo-OAAs (N/P 12, H_2O) formed with selected carriers 1284, 1285 and 1218 without (non) or with 0.5 equiv of monovalent DBCO agent PEG-1. Below: Corresponding representative TEM images of the pDNA lipo-OAAs (scale bars = 200 nm). Measured by Özgür Öztürk (LMU Pharmaceutical Biotechnology).

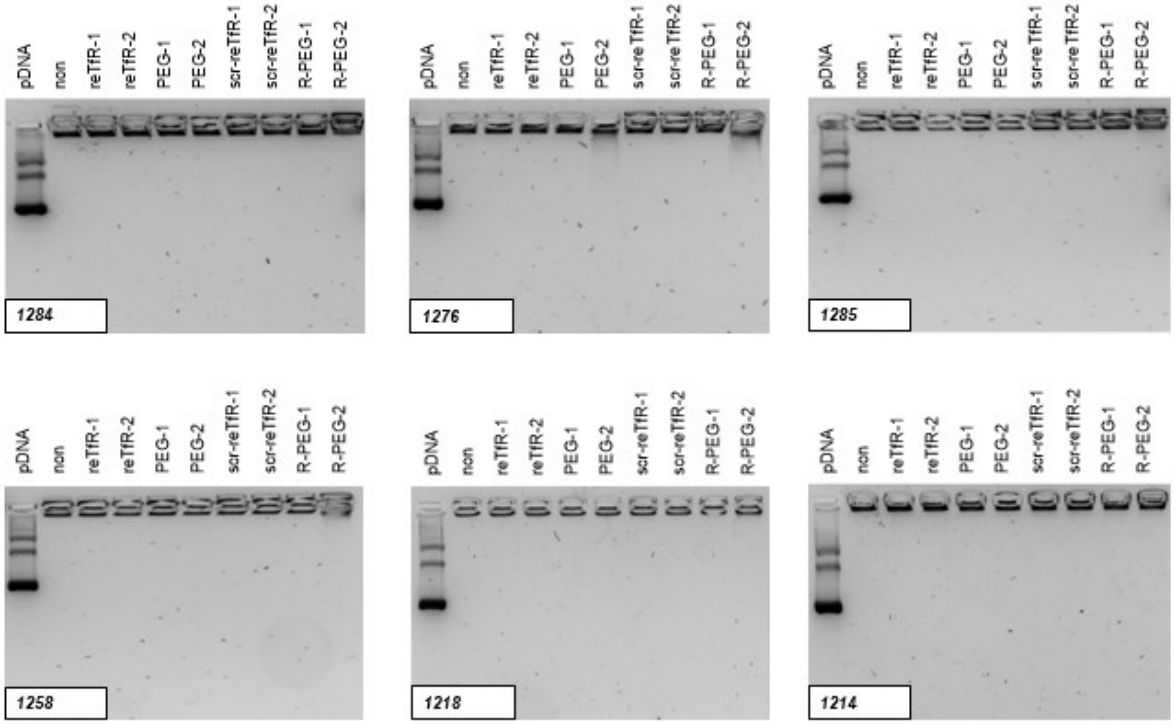

Figure 6 Standard agarose (1 % TBE buffer) gel shift of pDNA polyplexes formed at N/P 12 in HBG. Nonmodified polyplexes or polyplexes modified with 0.5 equiv of shielding and targeting agents were analyzed.

To investigate the influence of PEGylation on pDNA compaction (Figure 7), an EtBr exclusion assay was performed. The change of EtBr fluorescent signal from 20 % (related to uncompacted control pDNA) in case of nonmodified lipo-OAA

polyplexes to 40 % in case of all six PEG-1 modified polyplexes indicates a change toward less condensed pDNA polyplexes. This influence of PEG is consistent with previous observations [52, 67].

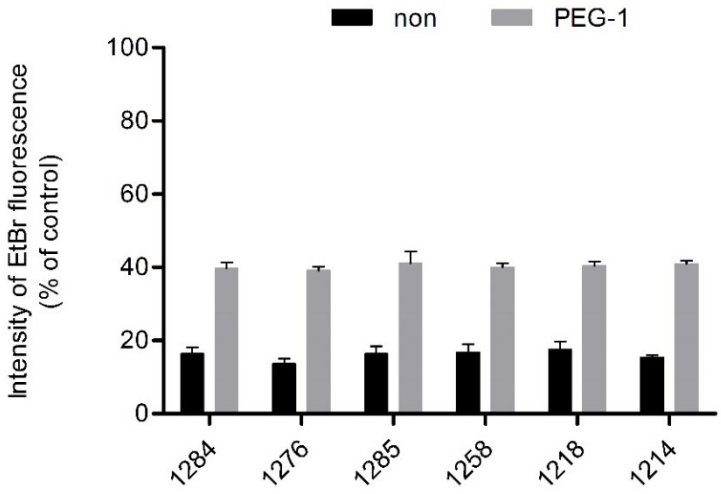

Figure 7 EtBr exclusion assay of pDNA polyplexes (N/P 12, HBG), unmodified or modified with 0.5 equiv of PEG-1 (mean ± sd, n = 3). Intensity of EtBr fluorescence is presented as percentage relative to free noncompacted pDNA. Experiment performed by Teoman Benli-Hoppe (LMU Pharmaceutical Biotechnology).

3.1.3 Gene Transfer Activity of TfR Targeted pDNA Polyplexes

Two TfR overexpressing cell lines, the hard to transfect human erythroleukemic suspension cell line K562 (Figure 8) and the adherent murine neuroblastoma cell line N2a (Figure 9) were transfected with the various surface modified pCMVLuc polyplexes and the resulting luciferase gene expression was measured after 24 h. In parallel, the metabolic cell activities were evaluated (Figure 10). None of the

tested formulations showed significant cytotoxicity; only polyplexes of lipo-OAAs 1276 and 1258 (both lacking the bioreducible ssbb linkage, containing the less lipophilic, more lytic DecA or NonOcA domains, respectively) had a slightly reduced metabolic activity in K562 cells, but still greater than 70 %. This is consistent with previous findings [33].

Luciferase activity in K562 cells (Figure 8) was increased by the reTfR ligand modification in all six lipo-OAA polyplexes to various extent (3 fold to 140 fold). In the majority of cases, reTfR-1 and reTfR-2 ligands mediated higher gene transfer efficiency than the scrambled control ligands scr-reTfR-1 and scr-reTfR-2, with the exception of 1276. The reTfR-2 modified polyplexes formed with the lipo-OAAs containing NonOcA, 1285 (ssbb) and 1258 (cys), displayed the highest transfection levels.

PEG-1/2, as well as R-PEG-1/2 were initially designed as expected negative controls. Interestingly, for some carriers these shielding agents enhanced gene transfer by a mechanism obviously different from TfR mediated uptake; PEG-1/2 strongly promoted transfection of 1284 polyplexes and also for 1258 and 1218 polyplexes to a lesser extent. R-PEG conjugates promoted transfection of 1284, 1285, 1258 or 1218 polyplexes, but to a lower extent.

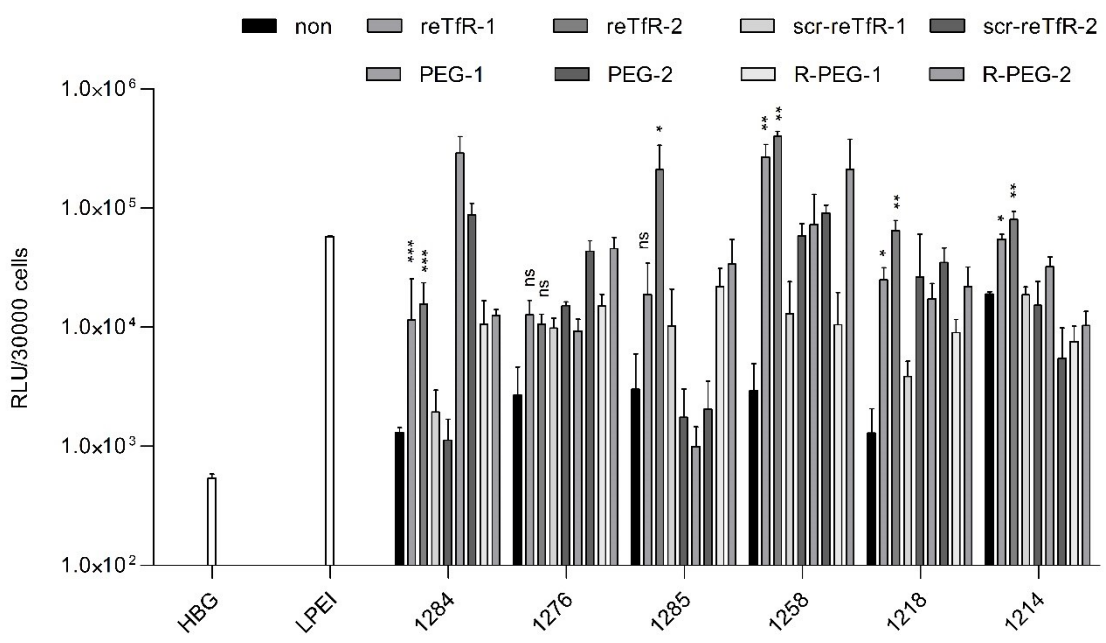

Figure 8 Luciferase gene transfer in K562 cells. pDNA polyplexes (200 ng pCMVLuc/well, N/P 12) modified with 0.5 equiv of shielding or targeting agents. Cells were incubated with polyplexes for 24 h in serum supplemented medium at 37 °C and harvested for the luciferase assay. LPEI (N/P 6) and HBG buffer served as positive and negative control, respectively. Results are presented as mean ± sd, n = 3. For the comparison of nonmodified polyplexes with reTfR-1 or reTfR-2 functionalized polyplexes, the statistical significance was determined by unpaired t-test (two-tailed analysis); ns, *p ≤ 0.05, **p ≤ 0.01 and ***p ≤ 0.001.

In the case of N2a cells, the transfection medium was replaced after 4 h, to emphasize any short term effects of surface modification on cell attachment and delivery before evaluating the transfection activity after 24 h (Figure 9). Apart from 1214 polyplexes, which generally transfected poorly, transfections were increased by incorporation of reTfR-1/2. In N2a cells, reTfR-2 modified polyplexes performed best with the ssbb-containing lipo-OAAs in the sequence of 1284 (DecA) > 1285 (NonOcA) > 1218 (OleA). The scrambled control ligands scr-reTfR-1 and scr-reTfR-2 again mediated lower transfection, with one very notable exception: the best transfections for 1285 polyplexes were obtained with scr-reTfR control modification. However, as described in section 3.1.2, these control polyplexes present micro-sized aggregates, which might explain their special properties. Similar to observation of K562 cell transfections, control PEGylation resulted in TfR–independent enhancement of transfection. This was especially pronounced for modification of 1284, 1285, 1258, and 1218 polyplexes with R-PEG-1 and/or R-PEG-2 (Figure 9).

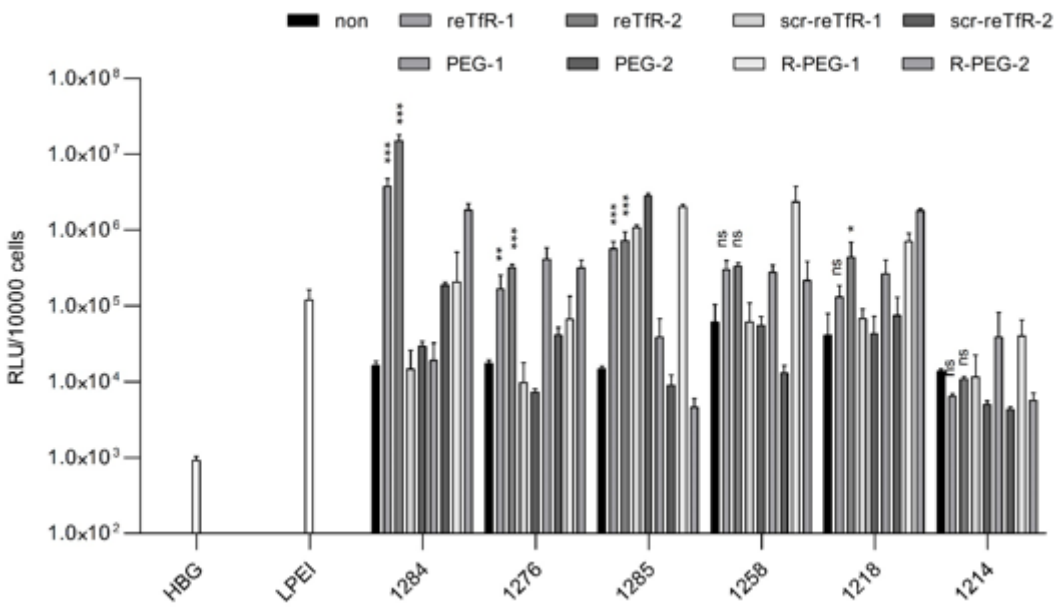

Figure 9 Luciferase gene transfer in N2a cells. pDNA polyplexes (200 ng pCMVLuc/well, N/P 12) modified with 0.5 equiv of shielding and targeting agents. Cells were incubated with polyplexes for 24 h in serum supplemented medium at 37 °C and harvested for the luciferase assay. The transfection medium was replaced after 4 h by fresh medium. LPEI (N/P 6) and HBG buffer served as positive and negative control, respectively. Results are presented as mean ± sd, n = 3. For the comparison of nonmodified polyplexes with reTfR-1 or reTfR-2 functionalized polyplexes, the statistical significance was determined by unpaired t-test (two-tailed analysis); ns, *p ≤ 0.05, **p ≤ 0.01 and ***p ≤ 0.001.

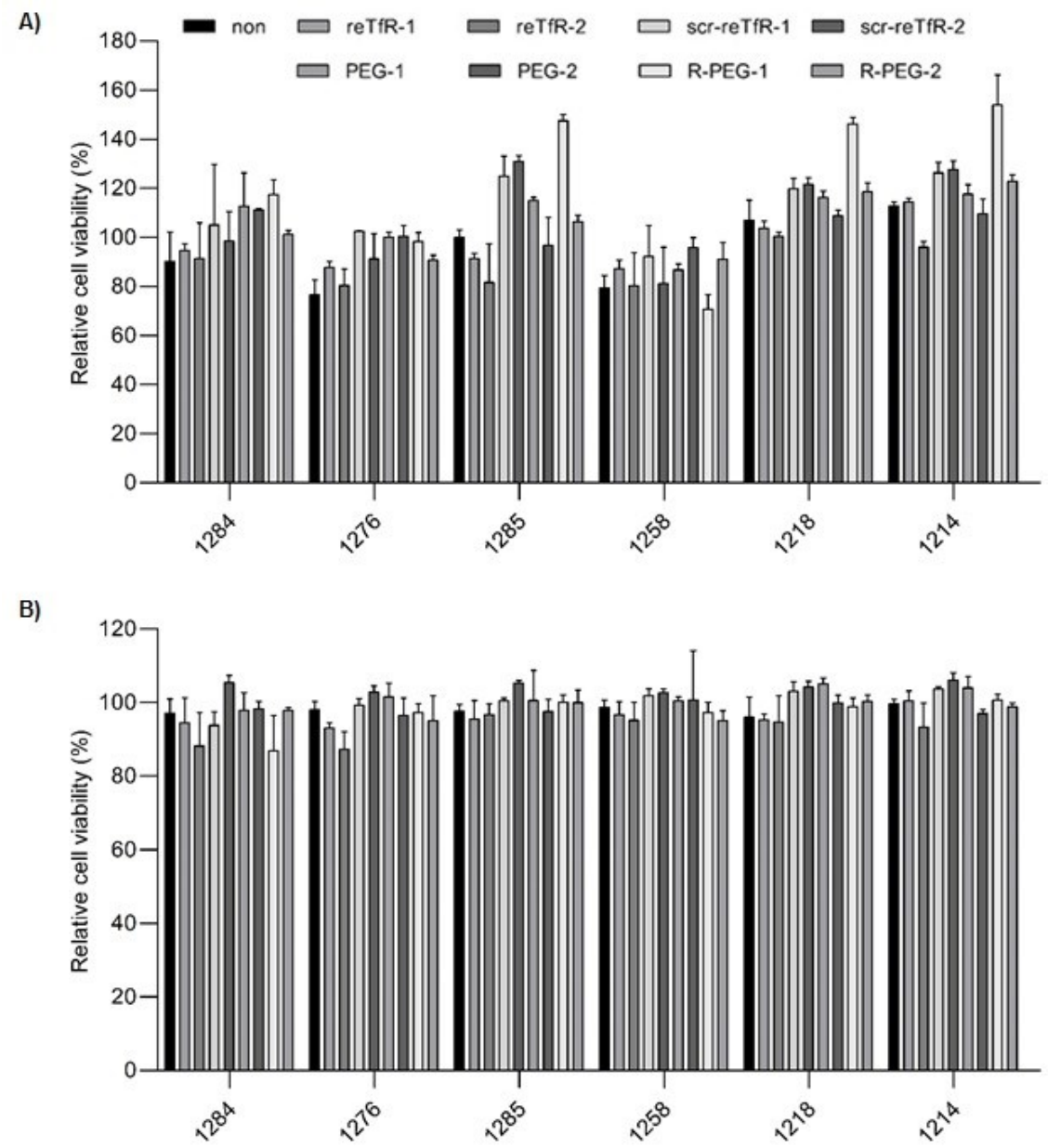

Figure 10 Metabolic activity of pDNA transfection in K562 (A) and N2a (B) cells were determined by the CellTiter-Glo® assay. Metabolic activities are presented as percentage relative to HBG buffer treated control cells (mean ± sd, n = 3).

The evaluation of six lipo-OAAs differing in their lipidic domains and redox-sensitive attachments and different control PEGylation reagents PEG-1/2 and R-PEG-1/2 shed also light on other important receptor unrelated effects of the gene

transfer process. While a proper receptor ligand interaction may mediate specific attachment and uptake into target cells, other parameters such as the choice of lipo-OAA and PEGylation conjugates can affect extracellular and intracellular biophysical stability of core pDNA polyplexes, influencing also endosomal escape of internalized pDNA nanoparticles and, after delivery into the nucleus, unpackaging of pDNA for subsequent transcription into mRNA. Our previous work on the tested lipo-OAAs had revealed a balancing act between favorable stability of pDNA polyplexes on the one hand, efficient endosomal escape and good intracellular pDNA release for transcription on the other hand. Lipo-OAAs containing fatty acids with chain lengths around C6 to C10 displayed maximum gene transfer around 500 fold higher gene expression than that of C18 lipo-OAA analogues [154]. The shorter fatty acids trigger increased endosomolytic activity, at the cost of reduced polyplex stability. Incorporation of hydrophilic PEG molecules is an additional measure to tune the polyplex stability. Consistent with previous observations [52, 67], PEGylation mediated slight polyplex decondensation detectable with an EtBr assay (Figure 7). Such a polyplex destabilization by PEG or R-PEG conjugates, shifting the amphiphilic properties of the carrier subunits towards higher hydrophilicity and aqueous solubility might be the cause of the unexpected high transfection efficiency of R-PEG conjugated 1284, 1285, 1258 or 1218 polyplexes. Noteworthy, our studies also revealed that TfR-specific delivery to a given target cell line, an optimized combination of lipo-OAA and ligand is required for the best transfection; reTfR-2/ 1258 or 1285 (both NonOcA-based) for K562 cells, and reTfR-2/ 1284 or 1285 (both ssbb based, DecA or NonOcA-based) for N2a cells.

To summarize the pDNA transfections, the reTfR ligands favorably promoted gene transfer efficiency in both K562 and N2a cells, with a small advantage when using the bivalent DBCO-containing conjugate reTfR-2.

3.1.4 Cellular Association of Functionalized pDNA Polyplexes

Cell association studies of reTfR-1 and reTfR-2 modified polyplexes were performed in K562 cells (Figure 11) and N2a cells (Figure 12). For further investigation, Cy5-labeled pDNA were transfected for 45 min and measured via fluorescence microscopy. Again, polyplexes (N/P 12) were formed in HBG. In K562 cells, overall reTfR modified polyplexes showed higher mean fluorescent intensity (MFI) than their negative controls, scr-reTfR and nonmodified polyplexes except 1285 polyplexes. Interestingly, R-PEG conjugated polyplexes 1284 and 1285 showed similar or even higher MFI than reTfR. On the other hand, scr-reTfR-1/2 had highest MFI for 1285.

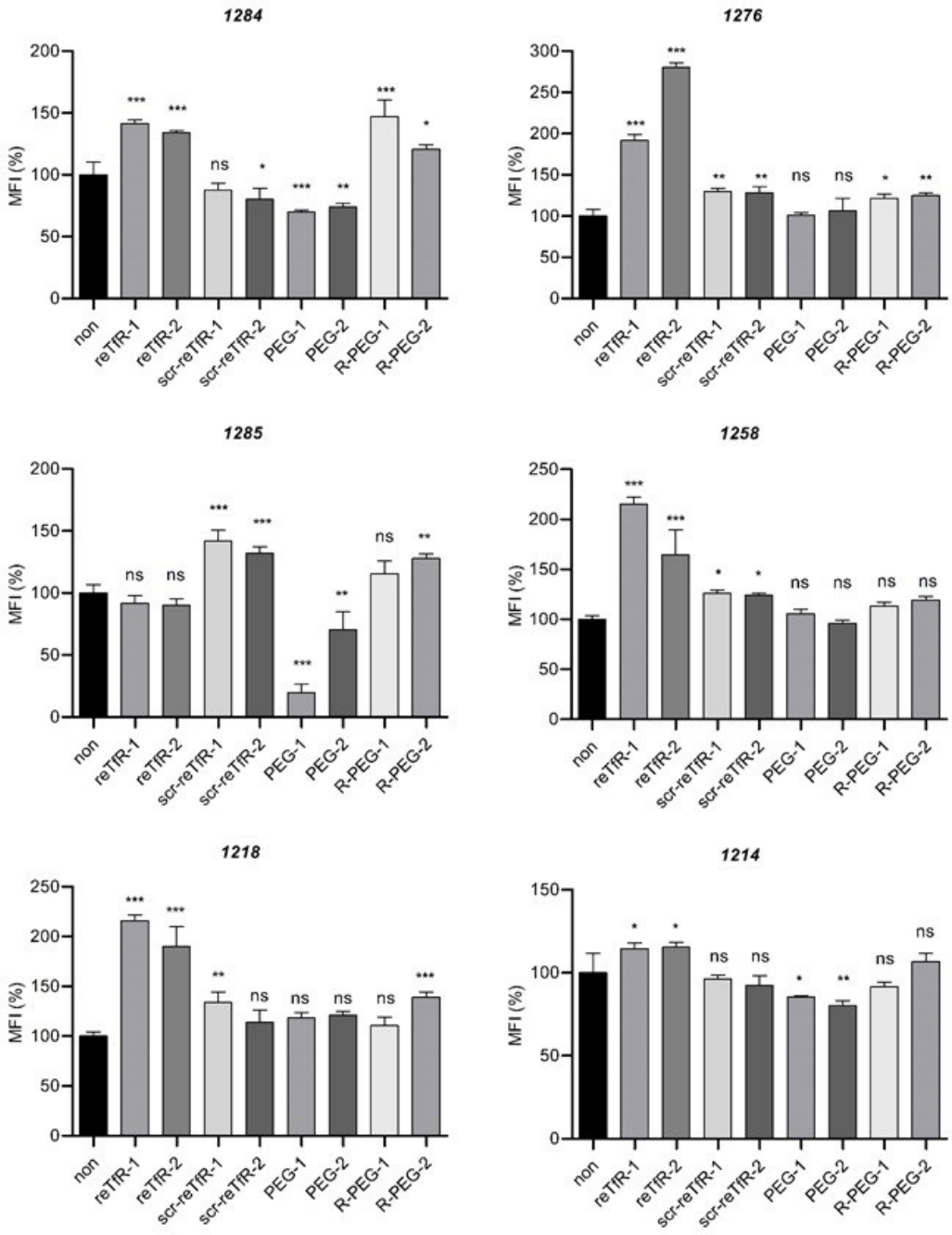

Figure 11 Cellular association of pDNA polyplexes with K562 cells. Cells were incubated with 200 ng/well, 20 % Cy5 labeled pDNA polyplexes (N/P12, 0.5 equiv of DBCO agent) for 45 min at 37 °C. Cellular association (MFI, % of nonmodified polyplexes) was measured by flow cytometry (mean ± sd, n = 3). The statistical significance was determined by one-way ANOVA; ns, *p ≤ 0.05, **p ≤ 0.01 and ***p ≤ 0.001.

In the case of N2a cells (Figure 12), reTfR modified 1276, 1218 and 1214 polyplexes showed higher cellular association than all of their controls and nonmodified forms. Additionally, reTfR-1/ 1284 had highest MFI compared to all other modified and nonmodified cases. The reTfR modified 1285 indicated higher MFI than PEG controls. Surprisingly, scr-reTfR-1 and R-PEG-1 also had higher cellular association. Polyplexes 1258 did not show any differences in all modified and nonmodified cases.

To evaluate of receptor mediated uptake, Tf receptor was blocked by 5 mg/ml free iron saturated hTf for 30 min on ice. Total of two polyplexes were chosen which were 1285 for K562 cells (Figure 13A) and 1284 for N2a cells (Figure 13B). Preincubation with hTf could block TfR and inhibit receptor mediated association of reTfR with K562 and N2a cells. These decreased associations were clear indicate of receptor specific uptake of reTfR ligands.

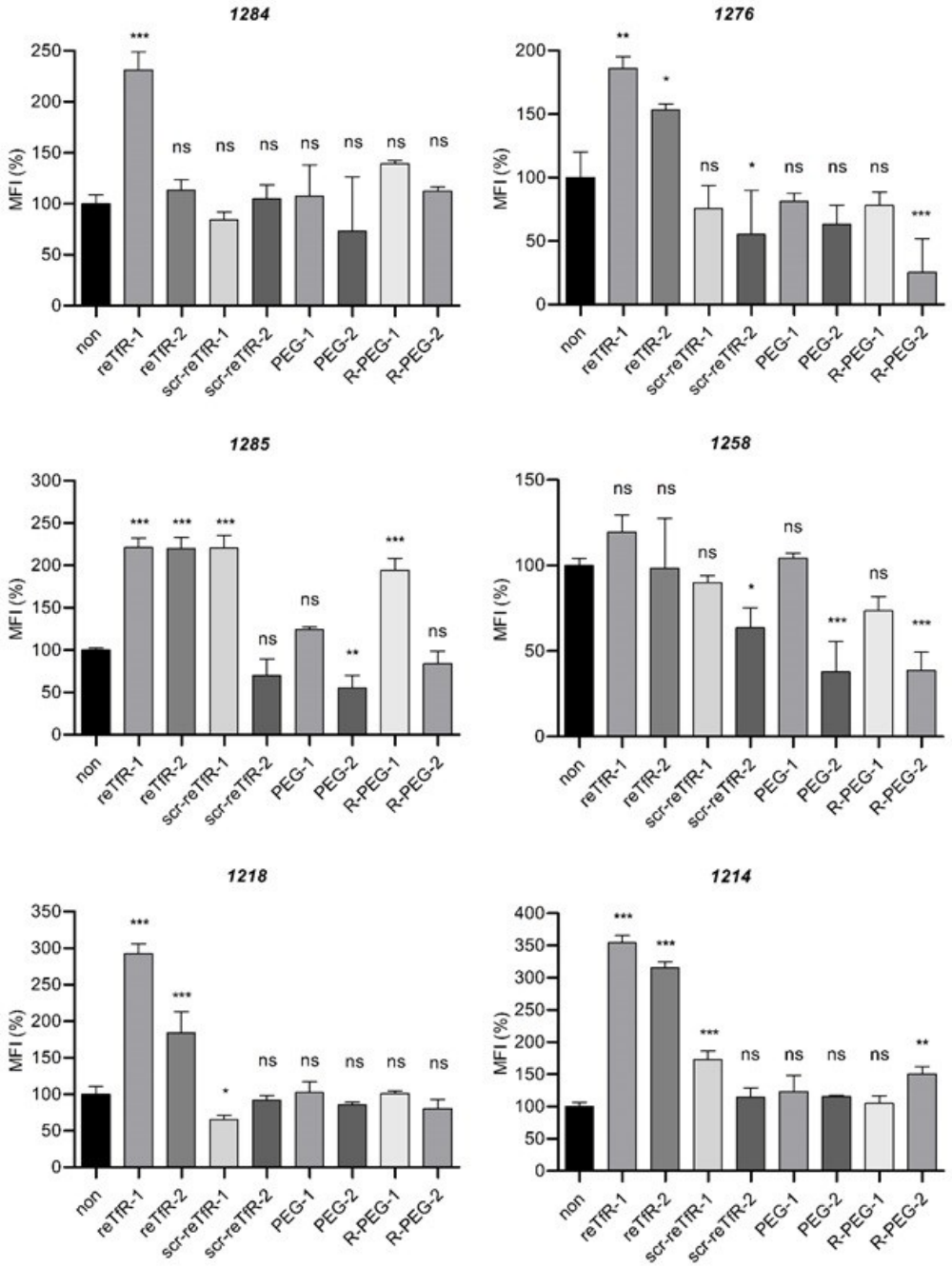

Figure 12 Cellular association of pDNA polyplexes with N2a cells. Cells were incubated with 200 ng/well, 20 % Cy5 labeled pDNA polyplexes (N/P 12, 0.5 equiv of DBCO agent) for 45 min at 37 °C. Cellular association (MFI, % of nonmodified polyplexes) was measured by flow cytometry (mean ± sd, n = 3). The statistical significance was determined by one-way ANOVA; ns, *p ≤ 0.05, **p ≤ 0.01 and ***p ≤ 0.001.

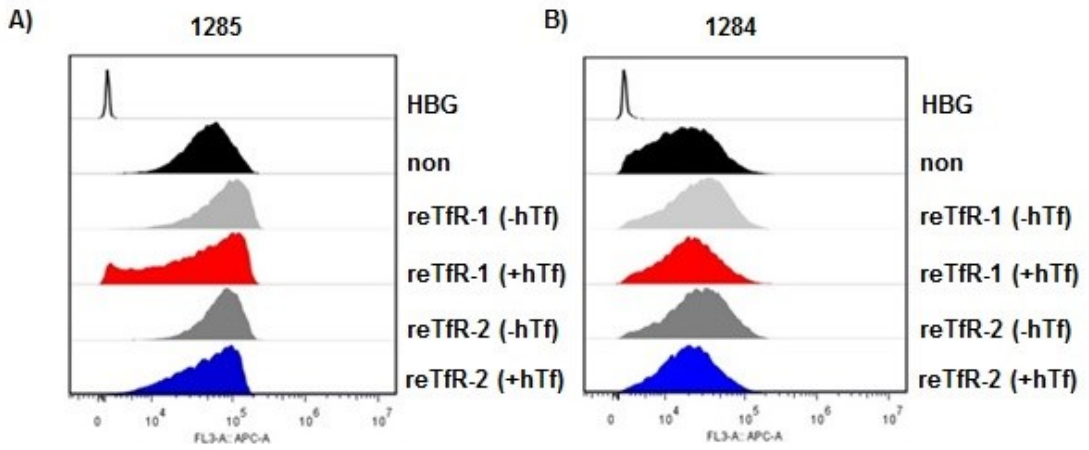

Figure 13 Cellular association of pDNA polyplexes. K562 cells (A) or N2a cells (B) were incubated with 200 ng/well, 20 % Cy5 labeled pDNA polyplexes for 45 min at 37 °C and measured by flow cytometry. TfR blockade performed with (+) or without (-) 5 mg/ml free iron saturated hTf for 30 min at 4°C prior to addition of polyplexes to cells. Data are presented as histograms of cells (x-axis, increasing Cy5 fluorescence intensity; y-axis, the number of cells).

According to the results, association of K562 cells was more complex than N2a cells. This complexity can be caused by cellular differences. It is not surprising that cell associations (which also may include unspecific cell binding only) and gene transfer efficiencies only correlate in part; gene transfer also depends on efficient intracellular uptake, endosomal escape and/or delivery into the cell nucleus as well as transcription. However, in both cases of 1285 reTfR and 1284 reTfR polyplexes, which are potent reTfR-enhanced transfection agents in K562 cells or N2a cells, respectively, a blockade of TfR by pre-incubation with iron saturated hTf reduced the cellular association of polyplexes (Figure 13). These results support the hypothesis of a Tf receptor-mediated gene transfer process of these reTfR polyplexes.

3.2 Transferrin Receptor Targeted LNPs

3.2.1 Design of hTf Targeted LNPs

Unfortunately, there is no single perfect way or vector to transport nucleic acids. Currently, a wide variety of non-viral vectors have been studied to increase transfection efficiency, specificity and decrease cellular toxicity. One of such vector system is LNPs that have recently provided new opportunities for nucleic acid therapies [166-168]. Therefore, hTf targeted LNPs were investigated to enhance pDNA transfection efficiency and specific cellular uptake in this thesis.

As first step, pDNA-LNPs were prepared as shown in Figure 14. Several components were utilized to construct of LNPs. Cationic lipid is the key component to encapsulate nucleic acids [169]. Positive charged cationic lipids easily bind to negative charged nucleic acids [170]. Previously, 1,2-dioleoyl-3-trimethyl-ammoniumpropane (DOTAP) was often used as a permanently positive charged lipid [171]. However, permanently positive charge has handicaps such as not being well tolerable *in vivo* and low transfection efficiency due to the limited nucleic acid release ability in the cell [58]. To address this issue, MC3 has been previously introduced as cationizable lipid [172]. In the current work, LNPs containing the ionizable lipooligomer CLO3 were generated based on the protocol by Franziska Haase (LMU Pharmaceutical Biotechnology). For pDNA delivery, various phospholipids are being used as a helper lipid such as DOPE to facilitate LNPs formation. DOPE containing LNPs achieved high transfection efficiency properties *in vivo* [56]. Other component of LNPs is cholesterol that enhances stability of nanoparticles and promotes endosomal escape [173]. PEG lipids also known as PEGylated lipids with lipid moiety such as DMG are used to

enhance delivery efficiency *in vivo* and had showed benefit to cellular uptake and endosomal escape of LNPs [174, 175]. Besides from all these components, PEG conjugated DSPE also used due its biocompatibility, biodegradability [176] and amphiphilic property, which makes DSPE-PEG able to interact with various materials to enhance specificity [177]. For these reasons, DSPE-PEG with azido group was used in this study for post functionalization with DBCO agents via click chemistry same as previously mentioned polyplexes in section 3.1.1.

As second step, LNPs were functionalized by targeting agent (Figure 14). The 80 kDa human transferrin protein was used as a targeting agent and it was modified by DBCO-PEG_{12} by Teoman Benli-Hoppe (LMU Pharmaceutical Biotechnology). Tf from human plasma was modified by coupling with 2 equiv of DBCO-PEG_{12}-NHS ester. DBCO amount linked to hTf is expected to be around 1.5 equiv click reaction between DBCO in hTf ligand and azide units in LNPs provides selectivity.

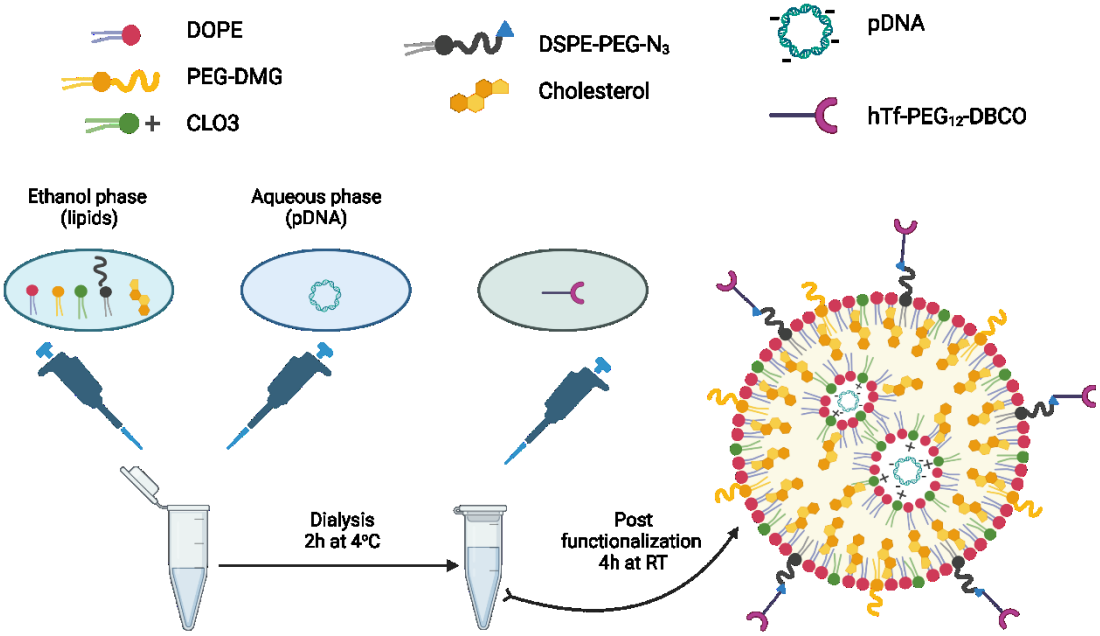

Figure 14 Formation of pDNA LNPs in a two-step process. LNPs were prepared by mixing lipids in ethanol phase and pDNA in aqueous phase, then post functionalizated with hTf ligand. Created with BioRender.com.

3.2.2 Physicochemical Characterization of Functionalized pDNA LNPs

For all following LNP studies, plasmid pCMVLuc was also used as nucleic acid cargo. The LNP formulations were prepared by mixing one volume of lipids and oligomers on ethanol (cholesterol:DOPE:PEG-DMG:DSPE-PEG-N_3:CLO3 at 45:20:**2**:**3**:**30** (2:3) or 45:20:**1**:**4**:30 (1:4) mole ratio). The N/P ratio of 9 for CLO3 and 4.5 for MC3 were used. Three volumes of pDNA (200 ng/well) containing citrate buffer solutions were mixed with lipid mixture. After dialyses in HEPES (pH 7.4) formulations were post functionalized with hTf-PEG_{12}-DBCO as described in

Figure 14. Nanoparticle size and zeta potential of LNP formulations were characterized by DLS and ELS (Figure 15).

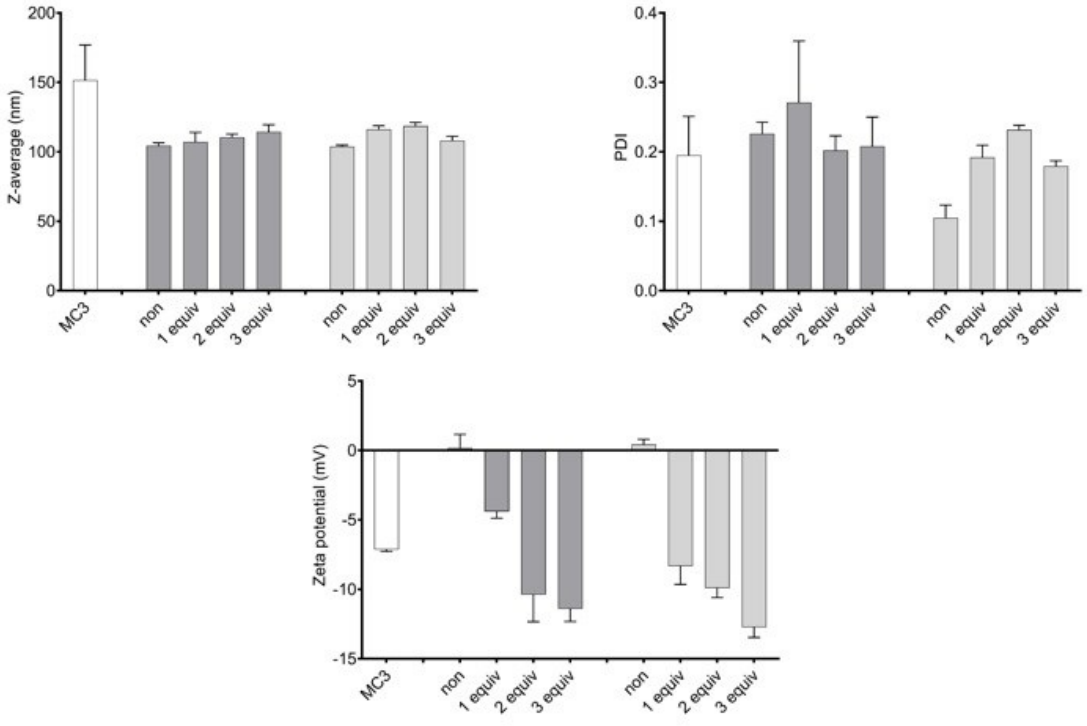

Figure 15 Particle size (Z-average), zeta potential and PDI values of pDNA LNPs (formed at N/P 9), nonmodified or modified with 1, 2 and 3 equiv of targeting agents, were measured by DLS and ELS (mean ± sd, n = 3). Dark gray bars and light gray represent 2:3 ratio and 1:4 ratio of PEG-DMG:DSPE-PEG-N_3, respectively.

The nonmodified 2:3 and 1:4 LNPs formed almost same sized particles, 104 and 103 nm diameter with neutral zeta potential, respectively. Their PDI were around 0.2, indicating well-formed particles. The hTf modified 2:3 LNPs have size between 107 and 115 nm. The charge of modified 2:3 LNPs gradually decreased with increased equiv of hTf from -4 to -11 mV. They displayed low PDI only 1

equiv hTf had relatively high PDI. The ratio of PEG-DMG and DSPE-PEG-N_3 did not change the size of hTf modified 1:4 LNPs which were sized between 108 and 116 nm. Similar to hTf modified 2:3 LNPs, the zeta potential of hTf modified LNP decreased from -8 to -13 with increased hTf equiv from 1 to 3 equiv, respectively. The hTf modified 1:4 LNPs had well-formed particles around 0.2 or less PDI values. Decrease of zeta potential without aggregation was explained by successfully conjugation of Tf ligands with LNPs.

Morphological characterization of LNPs was determined by TEM (Figure 16). The TEM analysis revealed that nonmodified and hTf modified LNPs were spherical, densely packed and mostly uniform particles with the diameter in the range of 70 to 76 nm. DLS results showed slightly larger particles than TEM results which is explainable by liquid layer around the particles, drying process during staining of the TEM and high sensitivity of the DLS to small amount of aggregates and larger particles.

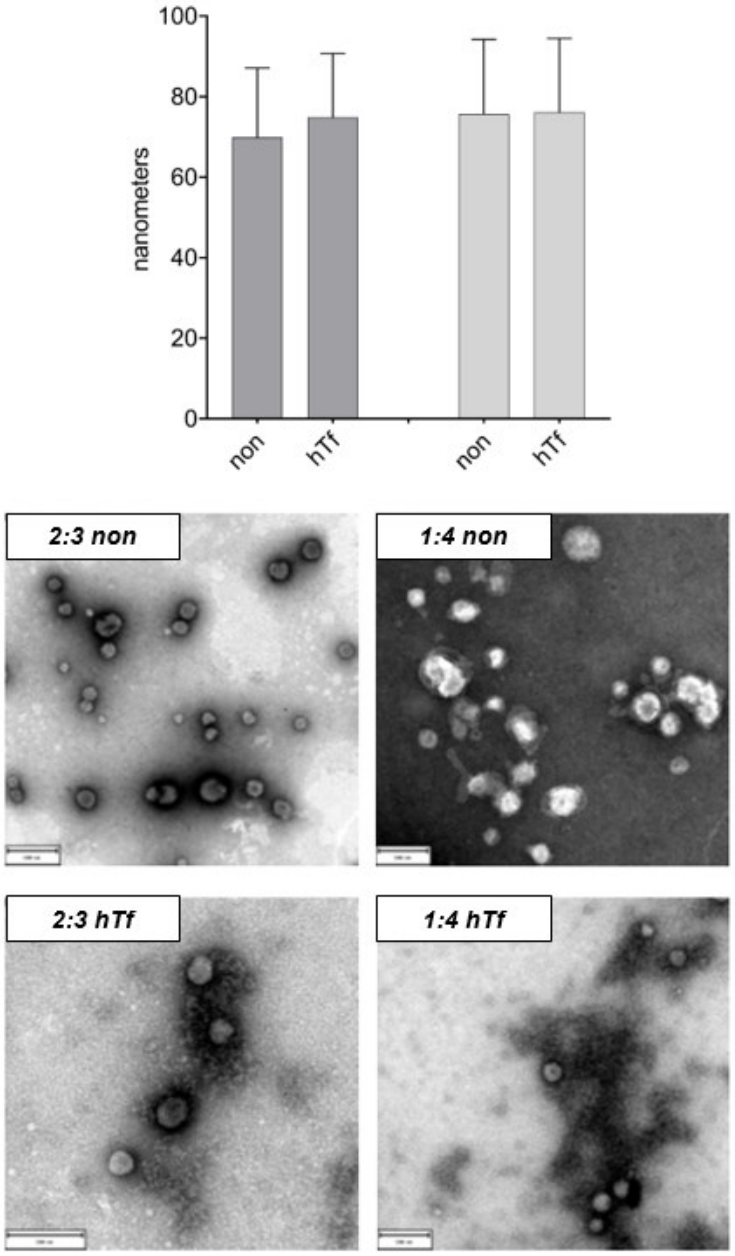

Figure 16 Top: TEM size data (diameter, nm) of pDNA LNPs (N/P 9, HEPES) with nonmodified LNPs or 3 equiv of hTf. Dark gray bars and light gray represent 2:3 ratio and 1:4 ratio of PEG-DMG:DSPE-PEG-N_3, respectively. Below: Corresponding representative TEM images of the pDNA LNPs. (scale bars = 200 nm). Measured by Özgür Öztürk (LMU Pharmaceutical Biotechnology).

In further characterization of nontargeted and targeted LNPs, the pDNA binding activity was determined by agarose gel shift assay. The sufficient pDNA binding was observed in the nonmodified and hTf modified 2.3 and 1:4 LNP formulations with no mobility of complexed pDNA (Figure 17). Agarose gel shift assay showed that different ratio of PEG-DMG:DSPE-PEG-N_3 or different equiv of hTf had high binding ability and stability with pDNA cargo.

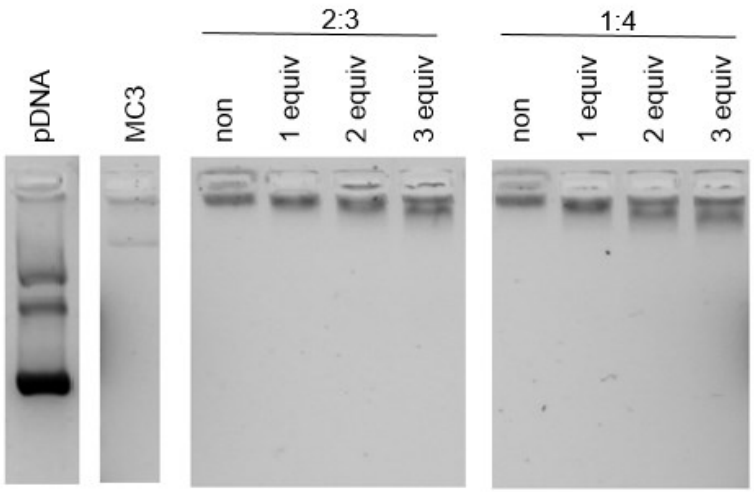

Figure 17 Standard agarose (1 % TBE buffer) gel shift assay. pDNA LNPs, MC3 formed at N/P 9 and N/P 4.5 in HEPES, respectively. Nonmodified LNPs or hTf modified LNPs with 1, 2 and 3 equiv of targeting agents were analyzed.

3.2.3 Gene Transfer Activity of TfR Targeted pDNA LNPs

Two different ratio of PEG-DMG:DSPE-PEG-N_3 were chosen for investigation of pDNA delivery efficiency to nucleus with hTf conjugated LNPs. Therefore, TfR overexpressed K562 cells were transfected with nonmodified and hTf modified LNPs. The both nonmodified 2:3 and 1:4 LNPs showed higher transfection

efficiency than MC3 positive control (Figure 18). Oligomer CLO3 formed successful LNP particles to transfect pDNA even without targeting agent. Three different equiv were selected to determine optimum delivery with hTf modified LNPs according to molar ratio of DBCO-PEG_{12}-hTf to DSPC-PEG-N_3. For hTf modified 2:3 LNPs, transfection ability significantly increased as the increased equiv of the hTf from 1 to 3. The highest transfection efficiency was observed in 2:3 LNP with 3 equiv of hTf ($p < 0.0001$). When DSPE-PEG-N_3 content increased from 2:**3** to 1:**4** LNP formulations, transfection efficiency significantly increased by hTf however, there is no obvious differences between different equivs of hTf.

Cellular toxicity of LNPs was evaluated by CellTiter-Glo®. HEPES was used as a negative control. Cell viability of LNP was around 80 % with nonmodified and hTf modified LNP in K562 cells (Figure 19). These results clearly showed that LNPs with or without hTf ligand are nontoxic carriers.

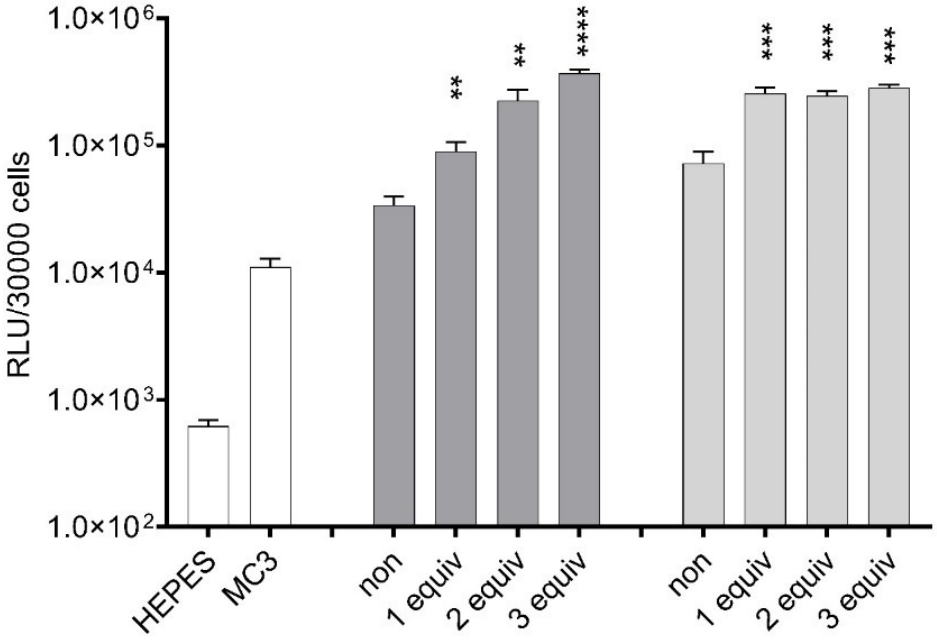

Figure 18 Luciferase gene transfer in K562 cells. pDNA LNPs (N/P 9, 200 ng pCMVLuc/well) modified with 1, 2 and 3 equiv of targeting agents. Cells were incubated with polyplexes for 24 h in serum supplemented medium at 37 °C and harvested for the luciferase assay. MC3 (N/P 4.5) and HEPES buffer served as positive and negative controls, respectively. Results are presented as mean ± sd, n = 3. For the comparison of nonmodified with hTf functionalized LNPs, the statistical significance was determined by unpaired t-test (two-tailed analysis); ns, *p ≤ 0.05, **p ≤ 0.01, ***p ≤ 0.001 and ****p≤ 0.0001. Dark gray bars and light gray represent 2:3 and 1:4 ratios of PEG-DMG:DSPE-PEG-N_3, respectively.

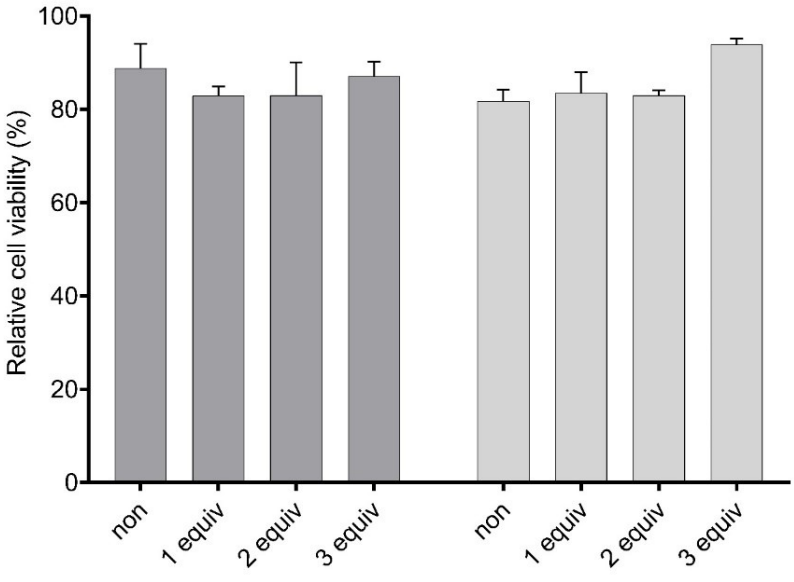

Figure 19 Metabolic activity of pDNA LNP transfection in K562 cells were determined by the CellTiter-Glo® assay. Metabolic activities are presented as percentage relative to HEPES buffer treated control cells (mean ± sd, n = 3). Dark gray bars and light gray represent 2:3 and 1:4 ratios of PEG-DMG:DSPE-PEG-N_3, respectively.

The amount of PEG in the LNPs can affect not only particle size and zeta potential but also particle stability by avoiding aggregation [178-180]. Additionally, to increase specificity of delivery, PEG-lipids can be interacted with specific lipids. DSPE-PEG-maleimide was used for chemically conjugation between maleimide group and MAdCAM-D1D2 ligand [181]. They clearly showed significantly improved therapeutic outcome with high specificity and without immune activation or liver toxicity. The total amount of PEG in the LNP was 2 % (PEG-DMG:DSPE-PEG-maleimide at 1.5:0.5 molar ratio). The percentage of LNP content is needed to optimized according to cell specific gene delivery [179, 182]. Additionally, type of the ligand also can affect LNP composition. For instance, FR targeted LNPs used total of 1.2 % PEG to enhance gene silencing in KB cells [183]. In this thesis,

3 or 4 % ligand interacted PEG (DSPE-PEG-N_3) were used in total of 5 % PEG (PEG-DMG + DSPE-PEG-N_3). We aimed to increase possibility of interaction between huge hTf ligand with LNPs via DBCO click chemistry. In case of 2:3 LNP formulations, modified LNPs increased transfection efficiency with increasing hTf equiv. On the other hand, 1:4 modified LNPs showed increased transfection efficiency compared to nonmodified LNPs however, increasing hTf equiv did not show similar gradual increase. Obviously, increased percentage of DSPC-PEG-N_3 hTf modified LNPs from 3 to 4 did not provide additional benefits to enhance transfection efficiency even with increased ligand equiv from 1 to 3.

MC3 is the promising candidate as an ionizable cationic lipid that is used in first FDA approved double stranded small interfering RNA delivering LNP (ONPATTRO, Patisiran) [184-186]. The among 56 amino lipid candidates, MC3 have been found the most active ionizable lipid [187]. However, undesired side effects of MC3 have been detected for chronic therapies [188]. In this thesis, the N/P 9 of cationizable lipooligomer CLO3 was chosen as a candidate for optimal particle formation. A high N/P ratio can increase the zeta potential, reduce the pDNA release capacity and cause low transfection efficiency [189, 190]. However, LNPs with selected N/P ratio showed well formed particles that were smaller than MC3. The new LNPs showed favorable *in vitro* transfection compared to the MC3 control, which however had not been optimized for pDNA delivery. hTf modified LNPs had negative zeta potential at both PEG-DMG:DSPE-PEG-N_3 ratios. The specificity of pDNA delivery with hTf modified LNPs is not only increased by receptor mediated uptake but also repulsion between negative charged hTf LNPs with negative charged cell membrane which decreases nonspecific interactions.

3.2.4 Cellular Association of Functionalized pDNA LNPs

To correlate findings of pDNA transfection activity with cellular association, 2:3 and 1:4 nonmodified and hTf modified LNPs incubated with K562 cells for 45 min and cell association evaluated by flow cytometer (Figure 20). The hTf protein is known specific uptake through TfR in K562 cells [142, 143]. Parallel results with pDNA transfection, hTf modified LNPs showed higher cell association than both 2:3 and 1:4 nonmodified LNPs. Interestingly, neither 2:3 nor 1:4 hTf modified LNPs displayed increased association by gradually increased equiv of hTf. Increased ligand equiv or DSPE-PEG-N_3 did not show any benefits with cellular association in hTf modified LNPs. Even, 1:4 hTf modified LNPs showed slightly decreased association with increasing ligand equiv but still higher than nonmodified LNPs. Parallel with section 3.1.4, 45 min incubation for association of ligand may not be sufficient for hard to transfect suspension K562 cells. The cell associations alone are not enough to explain endosomal escape and/or delivery into the cell nucleus as well as transcription. Increased transfection efficiency (Figure 18) may explained by higher endosomal escape capacity of 2:3 hTf modified LNPs with increased equiv of ligands. On the other hand, all hTf modified LNPs had negative zeta potential. The repulsion of the negative charged Tf and pDNA can cause pDNA release from complex into the cell cytoplasm and enhanced transfection efficiency apart from cellular association [191].

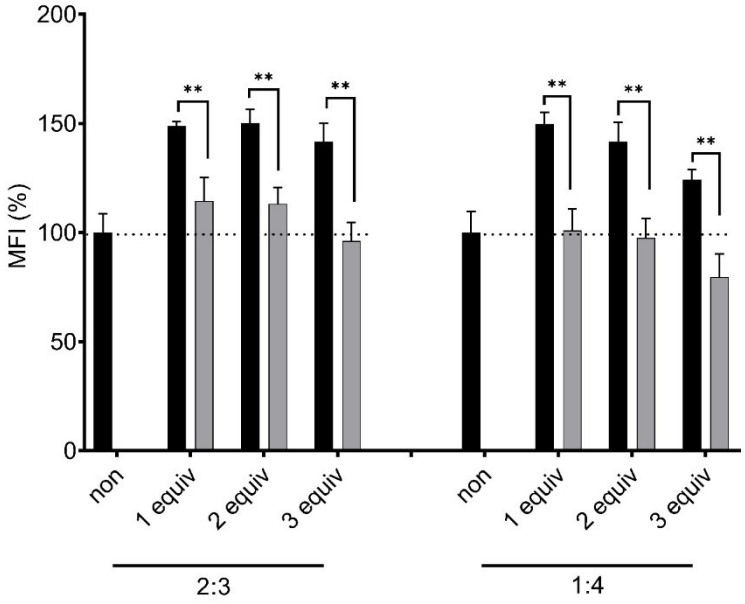

Figure 20 Cellular association of pDNA LNPs with K562 cells. Cells were incubated with 200 ng/well, 20 % Cy5 labeled pDNA LNPs (N/P 9, HEPES) for 45 min at 37 °C. TfR blockade performed with 5 mg/ml free iron saturated hTf for 30 min at 4°C prior to addition of LNPs to cells. Black and gray bars represent cellular association and TfR blockade, respectively. Cellular association (MFI, % of nonmodified polyplexes) was measured by flow cytometry (mean ± sd, n = 3). The statistical significance was determined by unpaired t-test (two-tailed analysis); ns, *p ≤ 0.05, **p ≤ 0.01 and ***p ≤ 0.001.

The receptor mediated uptake via hTf ligands was confirmed through competition experiment. K562 cells preincubated with iron saturated hTf (5 mg/ml) for 30 min on ice to block Tf receptor before LNPs added. Preincubation with iron saturated hTf reduced the cellular association of hTf modified LNPs in all equivs (Figure 20). These results verified that a TfR-mediated uptake is responsible for increased association and leads to higher transfection efficiency.

4. Summary

The therapy with nucleic acids showed great potential to cure life threatening, severe diseases especially for cancer. Non-viral gene delivery is a promising alternative to the classical method of viral gene delivery. However, non-viral nanocarriers need to be improved in several aspects such as suitable size, high stability outside of the cells, low affinity to blood components, high affinity to target cells, efficient uptake, successful endosomal escape and finally disassembly inside the cells. Current developments and increased knowledge in non-viral gene delivery systems open new doors to create optimum specialized nanocarriers. These synthetic carriers are able to be modified in different manners to improve their specificity and efficiency.

The first part of the thesis focuses on the transferrin receptor targeted pDNA delivery with previously design sequence defined T-shaped lipo-OAAs. In current study, only 12 amino acid length protease resistant synthetic retro-enantio TfR ligand was used as a targeting agent. Six lipo-OAAs differing in their lipidic domains and redox-sensitive attachments of lipid residues were tested in order to evaluate the impact of core polyplex stability on receptor-dependent gene transfer. The reTfR targeted pDNA polyplexes demonstrated receptor targeted gene delivery in TfR rich K562 and N2a cells with a small advantage when using the bivalent DBCO containing conjugate reTfR-2 compare to monovalent conjugate reTfR-1. Interestingly, each cell line has different lipo-OAAs for best transfection. The less stabilized NonOcA-OAA 1258 or 1285 / reTfR-2 was found to be suitable for pDNA delivery into erythroleukemic K562 cells and the ssbb-based bioreducible DecA- or NonOcA-OAAs 1284 or 1285 / reTfR-2 was best

suited for neuroblastoma N2a cells. The blockade of TfR by preincubation with iron saturated hTf reduced the cellular association of polyplexes which supports the hypothesis of a TfR-mediated gene transfer process of these reTfR polyplexes. Overall, transferrin receptor targeted sequence defined T-shaped lipo-OAA based specialized non-viral nanocarriers has been generated successfully.

In the second part of the thesis, hTf targeted LNPs were investigated to find optimum formulation for pDNA delivery. For this purpose, two different ratio of PEG-DMG:PEG-DSPE-N_3 and three different ligand equivalents were selected. Generated carriers analyzed in terms of size, zeta potential, morphology, stability, transfection efficiency and cellular association. Overall, hTf conjugated LNPs revealed higher transfection and association than nonmodified LNP formulations. In case of 2:3 LNP formulations, modified LNPs increased transfection efficiency with increasing hTf equiv. On the other hand, 1:4 modified LNPs showed increased transfection efficiency compared to nonmodified LNPs however, increasing hTf equiv did not show similar gradual increase. LNP formulations did not show any cellular toxicity *in vitro*. Most importantly, competition experiments support TfR-mediated uptake by reduced cellular association of hTf modified LNPs.

In summary, both 12 amino acid small protease resistant retro-enantio TfR binding peptide and 80 kDa serum iron transport protein transferrin showed notable power to enhance targeted gene delivery. Ligand conjugated lipo-OAAs and LNPs showed great potential to transfect pDNA cargo. These non-viral gene delivery systems might be candidates for further therapeutic developments.

5. Abbreviations

ASGPR	Asialoglyoprotein receptor
ATP	Adenosine 5′-triphosphate
BBB	Blood brain barrier
DAPI	4′,6-diamidino-2- phenylindole
DBCO	Dibenzocyclooctyne
DNA	Desoxyribonucleic acid
DecA	Decanoic acid
DLS	Dynamic light scattering
DMEM	Dulbecco's modified Eagle's medium
DMG-PEG	1,2-dimyristoyl-rac-glycero-3-methoxypolyethylene glycol-2000
DOPE	1,2-dioleoyl-sn-glycero-3-phosphorylethanolamine
DOTAP	1,2-dioleoyl-3-trimethyl- ammoniumpropane
DSPE-PEG-N_3	1,2-distearoyl-sn-glycero-3-phosphoethanolamine-N-[aazido(polyethylene gly-col)-2000]
DTT	Dithiothreitol
DTX	Docetaxel
EDTA	Ethylendiaminetetraacetic acid
EGF/EGFR	Epidermal growth factor / (receptor)
ELS	Electrophoretic light scattering
EPR	Enhanced permeability and retention
EtBr	Ethidium bromide
FA	Folate/Folic acid
FBS	Fetal bovine serum
FDA	Food and Drug Administration
FR	Folate receptor
G-ssbb	Glycine-disulfide block
HA	Hyaluronic acid
HBG	Hepes-buffered glucose
HEPES	N-(2-Hydroxethyl) piperazine-N'-(2-ethansulfonic acid)
HES	Hydroxyethyl starch
hTf	Human transferrin
kDa	Kilodalton
lipo-OOAs	Lipo-oligoaminoamides
LNPs	Lipid nanoparticles
LPEI	Linear polyethylenimine
MC3	D-Lin-MC3-DMA
MFI	Mean fluorescent intensity
mM	Millimolar
mRNA	Messenger RNA
mV	Millivolt
N/P	Nitrogen to phosphates ratio

nm	Nanometer
NLS	Nuclear localization signal
NonOcA	Nonamido octanoic acid
NPC	Nuclear pore complex
ns	Not significant
OAA	Oligoaminoamide
OleA	Oleic acid
PAS	Pro-Ala-Ser
PBS	Phosphate-buffered saline
pCMVLuc	Plasmid encoding for firefly luciferase
PDI	Polydispersity index
pDNA	Plasmid DNA
PEG	Polyethylene glycol
PEI	Polyethylenimine
pHPMA	Poly(N-(2-hydroxypropyl) methacrylamide)
PLL	Poly-L-lysine
reTfR	Retro-enantio-Transferrin receptor binding peptide
RGD	Arginine–glycine–aspartic acid
RLU	Relative light units
RNA	Ribonucleic acid
RT	Room temperature
siRNA	Small interfering RNA
SPS	Solid-phase synthesis
STOTDA	Succinyl-trioxa-tridecandiamine
TBE	Tris-boric acid-EDTA buffer
TEM	Transmission electron microscopy
Tf	Transferrin
TfR	Transferrin receptor

6. References

1. Watson, J.D. and F.H. Crick, *Molecular structure of nucleic acids; a structure for deoxyribose nucleic acid.* Nature, 1953. **171**(4356): p. 737-8.
2. Wilkins, M.H., A.R. Stokes, and H.R. Wilson, *Molecular structure of deoxypentose nucleic acids.* Nature, 1953. **171**(4356): p. 738-40.
3. Franklin, R.E. and R.G. Gosling, *Molecular configuration in sodium thymonucleate.* Nature, 1953. **171**(4356): p. 740-1.
4. Crick, F.H., *On protein synthesis.* Symp Soc Exp Biol, 1958. **12**: p. 138-63.
5. Crick, F.H., *The origin of the genetic code.* J Mol Biol, 1968. **38**(3): p. 367-79.
6. Crick, F., *Central dogma of molecular biology.* Nature, 1970. **227**(5258): p. 561-3.
7. Friedmann, T. and R. Roblin, *Gene therapy for human genetic disease?* Science, 1972. **175**(4025): p. 949-55.
8. Mulligan, R.C., *The basic science of gene therapy.* Science, 1993. **260**(5110): p. 926-32.
9. Wan, P.K., A.J. Ryan, and L.W. Seymour, *Beyond cancer cells: Targeting the tumor microenvironment with gene therapy and armed oncolytic virus.* Mol Ther, 2021. **29**(5): p. 1668-1682.
10. Hacker, U.T., et al., *Towards Clinical Implementation of Adeno-Associated Virus (AAV) Vectors for Cancer Gene Therapy: Current Status and Future Perspectives.* Cancers (Basel), 2020. **12**(7).
11. Touchot, N. and M. Flume, *Early Insights from Commercialization of Gene Therapies in Europe.* Genes (Basel), 2017. **8**(2).
12. Stein, C.A. and D. Castanotto, *FDA-Approved Oligonucleotide Therapies in 2017.* Mol Ther, 2017. **25**(5): p. 1069-1075.
13. Greco, O., et al., *Cancer gene therapy: 'delivery, delivery, delivery'.* Front Biosci, 2002. **7**: p. d1516-24.
14. Barrett, D.M., *Gene, Cell, and RNA Therapy Landscape: Q2 2021*. 2021: American Society of Gene and Cell Therapy.
15. Opalinska, J.B. and A.M. Gewirtz, *Nucleic-acid therapeutics: basic principles and recent applications.* Nat Rev Drug Discov, 2002. **1**(7): p. 503-14.
16. Wirth, T., N. Parker, and S. Yla-Herttuala, *History of gene therapy.* Gene, 2013. **525**(2): p. 162-9.
17. *Gene Therapy Clinical Trials Worldwide*. [cited 2022 May]; Available from: https://a873679.fmphost.com/fmi/webd/GTCT.
18. Girod, A., et al., *Genetic capsid modifications allow efficient re-targeting of adeno-associated virus type 2.* Nat Med, 1999. **5**(12): p. 1438.
19. Wu, P., et al., *Mutational analysis of the adeno-associated virus type 2 (AAV2) capsid gene and construction of AAV2 vectors with altered tropism.* J Virol, 2000. **74**(18): p. 8635-47.
20. Soong, N.W., et al., *Molecular breeding of viruses.* Nat Genet, 2000. **25**(4): p. 436-9.

21. Lavillette, D., S.J. Russell, and F.L. Cosset, *Retargeting gene delivery using surface-engineered retroviral vector particles.* Curr Opin Biotechnol, 2001. **12**(5): p. 461-6.
22. Rayaprolu, V., et al., *Length of encapsidated cargo impacts stability and structure of in vitro assembled alphavirus core-like particles.* J Phys Condens Matter, 2017. **29**(48): p. 484003.
23. Hacein-Bey-Abina, S., et al., *Insertional oncogenesis in 4 patients after retrovirus-mediated gene therapy of SCID-X1.* J Clin Invest, 2008. **118**(9): p. 3132-42.
24. Wilson, J.M., *Lessons learned from the gene therapy trial for ornithine transcarbamylase deficiency.* Mol Genet Metab, 2009. **96**(4): p. 151-7.
25. Wolff, J.A., et al., *Direct gene transfer into mouse muscle in vivo.* Science, 1990. **247**(4949 Pt 1): p. 1465-8.
26. Ulmer, J.B., et al., *Heterologous protection against influenza by injection of DNA encoding a viral protein.* Science, 1993. **259**(5102): p. 1745-9.
27. Yang, N.S., et al., *In vivo and in vitro gene transfer to mammalian somatic cells by particle bombardment.* Proc Natl Acad Sci U S A, 1990. **87**(24): p. 9568-72.
28. Rols, M.P., et al., *In vivo electrically mediated protein and gene transfer in murine melanoma.* Nat Biotechnol, 1998. **16**(2): p. 168-71.
29. Mintzer, M.A. and E.E. Simanek, *Nonviral vectors for gene delivery.* Chem Rev, 2009. **109**(2): p. 259-302.
30. Schaffert, D. and E. Wagner, *Gene therapy progress and prospects: synthetic polymer-based systems.* Gene Ther, 2008. **15**(16): p. 1131-8.
31. Pichon, C., L. Billiet, and P. Midoux, *Chemical vectors for gene delivery: uptake and intracellular trafficking.* Curr Opin Biotechnol, 2010. **21**(5): p. 640-5.
32. Wagner, E., *Programmed drug delivery: nanosystems for tumor targeting.* Expert Opin Biol Ther, 2007. **7**(5): p. 587-93.
33. Klein, P.M., et al., *Precise redox-sensitive cleavage sites for improved bioactivity of siRNA lipopolyplexes.* Nanoscale, 2016. **8**(42): p. 18098-18104.
34. Bloomfield, V.A., *DNA condensation by multivalent cations.* Biopolymers, 1997. **44**(3): p. 269-82.
35. Felgner, P.L., et al., *Nomenclature for synthetic gene delivery systems.* Hum Gene Ther, 1997. **8**(5): p. 511-2.
36. Choi, H.S., et al., *Design considerations for tumour-targeted nanoparticles.* Nat Nanotechnol, 2010. **5**(1): p. 42-7.
37. Yuan, F., et al., *Vascular permeability in a human tumor xenograft: molecular size dependence and cutoff size.* Cancer Res, 1995. **55**(17): p. 3752-6.
38. Smrekar, B., et al., *Tissue-dependent factors affect gene delivery to tumors in vivo.* Gene Ther, 2003. **10**(13): p. 1079-88.
39. Cabral, H., et al., *Accumulation of sub-100 nm polymeric micelles in poorly permeable tumours depends on size.* Nat Nanotechnol, 2011. **6**(12): p. 815-23.
40. Piest, M. and J.F.J. Engbersen, *Effects of charge density and hydrophobicity of poly(amido amine)s for non-viral gene delivery.* J Control Release, 2010. **148**(1): p. 83-90.

41. Russ, V., et al., *Improved in vivo gene transfer into tumor tissue by stabilization of pseudodendritic oligoethylenimine-based polyplexes.* J Gene Med, 2010. **12**(2): p. 180-93.
42. Philipp, A., et al., *Hydrophobically modified oligoethylenimines as highly efficient transfection agents for siRNA delivery.* Bioconjug Chem, 2009. **20**(11): p. 2055-61.
43. Fröhlich, T., et al., *Stabilization of polyplexes via polymer crosslinking for efficient siRNA delivery.* Eur J Pharm Sci, 2012. **47**(5): p. 914-20.
44. Wagner, K.G. and R. Arav, *On the interaction of nucleotides with poly-L-lysine and poly-L-arginine. I. The influence of the nucleotide base on the binding behavior.* Biochemistry, 1968. **7**(5): p. 1771-7.
45. Farber, F.E., J.L. Melnick, and J.S. Butel, *Optimal conditions for uptake of exogenous DNA by Chinese hamster lung cells deficient in hypoxanthine-guanine phosphoribosyltransferase.* Biochim Biophys Acta, 1975. **390**(3): p. 298-311.
46. Wu, G.Y. and C.H. Wu, *Receptor-mediated gene delivery and expression in vivo.* J Biol Chem, 1988. **263**(29): p. 14621-4.
47. Wagner, E., et al., *Transferrin-polycation-DNA complexes: the effect of polycations on the structure of the complex and DNA delivery to cells.* Proc Natl Acad Sci U S A, 1991. **88**(10): p. 4255-9.
48. Plank, C., et al., *Branched cationic peptides for gene delivery: role of type and number of cationic residues in formation and in vitro activity of DNA polyplexes.* Hum Gene Ther, 1999. **10**(2): p. 319-32.
49. Parker, A.L., et al., *Enhanced gene transfer activity of peptide-targeted gene-delivery vectors.* J Drug Target, 2005. **13**(1): p. 39-51.
50. Wadhwa, M.S., et al., *Peptide-mediated gene delivery: influence of peptide structure on gene expression.* Bioconjug Chem, 1997. **8**(1): p. 81-8.
51. Adami, R.C., et al., *Stability of peptide-condensed plasmid DNA formulations.* J Pharm Sci, 1998. **87**(6): p. 678-83.
52. Kos, P., et al., *Histidine-rich stabilized polyplexes for cMet-directed tumor-targeted gene transfer.* Nanoscale, 2015. **7**(12): p. 5350-62.
53. Fröhlich, T., et al., *Structure-activity relationships of siRNA carriers based on sequence-defined oligo (ethane amino) amides.* J Control Release, 2012. **160**(3): p. 532-41.
54. Zhao, Y. and L. Huang, *Lipid nanoparticles for gene delivery.* Adv Genet, 2014. **88**: p. 13-36.
55. Kulkarni, J.A., P.R. Cullis, and R. van der Meel, *Lipid Nanoparticles Enabling Gene Therapies: From Concepts to Clinical Utility.* Nucleic Acid Ther, 2018. **28**(3): p. 146-157.
56. Kulkarni, J.A., et al., *Design of lipid nanoparticles for in vitro and in vivo delivery of plasmid DNA.* Nanomedicine, 2017. **13**(4): p. 1377-1387.
57. Xu, R., X.L. Wang, and Z.R. Lu, *New amphiphilic carriers forming pH-sensitive nanoparticles for nucleic acid delivery.* Langmuir, 2010. **26**(17): p. 13874-82.
58. Kedmi, R., N. Ben-Arie, and D. Peer, *The systemic toxicity of positively charged lipid nanoparticles and the role of Toll-like receptor 4 in immune activation.* Biomaterials, 2010. **31**(26): p. 6867-75.

59. Üzgün, S., et al., *PEGylation improves nanoparticle formation and transfection efficiency of messenger RNA.* Pharm Res, 2011. **28**(9): p. 2223-32.
60. Mislick, K.A. and J.D. Baldeschwieler, *Evidence for the role of proteoglycans in cation-mediated gene transfer.* Proc Natl Acad Sci U S A, 1996. **93**(22): p. 12349-54.
61. Suk, J.S., et al., *PEGylation as a strategy for improving nanoparticle-based drug and gene delivery.* Adv Drug Deliv Rev, 2016. **99**(Pt A): p. 28-51.
62. Khargharia, S., et al., *PEG length and chemical linkage controls polyacridine peptide DNA polyplex pharmacokinetics, biodistribution, metabolic stability and in vivo gene expression.* J Control Release, 2013. **170**(3): p. 325-33.
63. Kursa, M., et al., *Novel shielded transferrin-polyethylene glycol-polyethylenimine/DNA complexes for systemic tumor-targeted gene transfer.* Bioconjug Chem, 2003. **14**(1): p. 222-31.
64. Merkel, O.M., et al., *Stability of siRNA polyplexes from poly(ethylenimine) and poly(ethylenimine)-g-poly(ethylene glycol) under in vivo conditions: effects on pharmacokinetics and biodistribution measured by Fluorescence Fluctuation Spectroscopy and Single Photon Emission Computed Tomography (SPECT) imaging.* J Control Release, 2009. **138**(2): p. 148-59.
65. Noga, M., et al., *Controlled shielding and deshielding of gene delivery polyplexes using hydroxyethyl starch (HES) and alpha-amylase.* J Control Release, 2012. **159**(1): p. 92-103.
66. Burke, R.S. and S.H. Pun, *Synthesis and characterization of biodegradable HPMA-oligolysine copolymers for improved gene delivery.* Bioconjug Chem, 2010. **21**(1): p. 140-50.
67. Morys, S., et al., *Influence of Defined Hydrophilic Blocks within Oligoaminoamide Copolymers: Compaction versus Shielding of pDNA Nanoparticles.* Polymers (Basel), 2017. **9**(4).
68. Heller, P., et al., *Introducing PeptoPlexes: polylysine-block-polysarcosine based polyplexes for transfection of HEK 293T cells.* Macromol Biosci, 2014. **14**(10): p. 1380-95.
69. Saifer, M.G., et al., *Selectivity of binding of PEGs and PEG-like oligomers to anti-PEG antibodies induced by methoxyPEG-proteins.* Mol Immunol, 2014. **57**(2): p. 236-46.
70. Tockary, T.A., et al., *Rod-to-Globule Transition of pDNA/PEG-Poly(l-Lysine) Polyplex Micelles Induced by a Collapsed Balance Between DNA Rigidity and PEG Crowdedness.* Small, 2016. **12**(9): p. 1193-200.
71. Vasiliu, T., et al., *In silico study of PEI-PEG-squalene-dsDNA polyplex formation: the delicate role of the PEG length in the binding of PEI to DNA.* Biomater Sci, 2021. **9**(19): p. 6623-6640.
72. Grun, M.K., et al., *PEGylation of poly(amine-co-ester) polyplexes for tunable gene delivery.* Biomaterials, 2021. **272**: p. 120780.
73. Beckert, L., et al., *Acid-labile pHPMA modification of four-arm oligoaminoamide pDNA polyplexes balances shielding and gene transfer activity in vitro and in vivo.* Eur J Pharm Biopharm, 2016. **105**: p. 85-96.

74. Morys, S., et al., *EGFR Targeting and Shielding of pDNA Lipopolyplexes via Bivalent Attachment of a Sequence-Defined PEG Agent.* Macromol Biosci, 2018. **18**(1).
75. Wu, Z. and T. Li, *Nanoparticle-Mediated Cytoplasmic Delivery of Messenger RNA Vaccines: Challenges and Future Perspectives.* Pharm Res, 2021. **38**(3): p. 473-478.
76. Kanamala, M., et al., *Dual pH-sensitive liposomes with low pH-triggered sheddable PEG for enhanced tumor-targeted drug delivery.* Nanomedicine (Lond), 2019. **14**(15): p. 1971-1989.
77. Ogris, M., et al., *DNA/polyethylenimine transfection particles: influence of ligands, polymer size, and PEGylation on internalization and gene expression.* AAPS PharmSci, 2001. **3**(3): p. E21.
78. Vetter, V.C. and E. Wagner, *Targeting nucleic acid-based therapeutics to tumors: Challenges and strategies for polyplexes.* J Control Release, 2022. **346**: p. 110-135.
79. Arap, W., R. Pasqualini, and E. Ruoslahti, *Cancer treatment by targeted drug delivery to tumor vasculature in a mouse model.* Science, 1998. **279**(5349): p. 377-80.
80. Schilb, A.L., et al., *Efficacy of Targeted ECO/miR-200c Nanoparticles for Modulating Tumor Microenvironment and Treating Triple Negative Breast Cancer as Non-invasively Monitored by MR Molecular Imaging.* Pharm Res, 2021. **38**(8): p. 1405-1418.
81. Vaidya, A.M., et al., *Systemic Delivery of Tumor-Targeting siRNA Nanoparticles against an Oncogenic LncRNA Facilitates Effective Triple-Negative Breast Cancer Therapy.* Bioconjug Chem, 2019. **30**(3): p. 907-919.
82. Oba, M., et al., *Cyclic RGD peptide-conjugated polyplex micelles as a targetable gene delivery system directed to cells possessing alphavbeta3 and alphavbeta5 integrins.* Bioconjug Chem, 2007. **18**(5): p. 1415-23.
83. Lei, Y., et al., *Glutathione-sensitive RGD-poly(ethylene glycol)-SS-polyethylenimine for intracranial glioblastoma targeted gene delivery.* J Gene Med, 2013. **15**(8-9): p. 291-305.
84. Egorova, A., et al., *Polycondensed Peptide Carriers Modified with Cyclic RGD Ligand for Targeted Suicide Gene Delivery to Uterine Fibroid Cells.* Int J Mol Sci, 2022. **23**(3).
85. Shi, B., M. Abrams, and L. Sepp-Lorenzino, *Expression of asialoglycoprotein receptor 1 in human hepatocellular carcinoma.* J Histochem Cytochem, 2013. **61**(12): p. 901-9.
86. Naidoo, S., et al., *Poly-L-Lysine-Lactobionic Acid-Capped Selenium Nanoparticles for Liver-Targeted Gene Delivery.* Int J Mol Sci, 2022. **23**(3).
87. Chen, J., et al., *A novel gene delivery system using EGF receptor-mediated endocytosis.* FEBS Lett, 1994. **338**(2): p. 167-9.
88. Xu, B., et al., *The contribution of poly-L-lysine, epidermal growth factor and streptavidin to EGF/PLL/DNA polyplex formation.* Gene Ther, 1998. **5**(9): p. 1235-43.
89. Li, Z., et al., *Identification and characterization of a novel peptide ligand of epidermal growth factor receptor for targeted delivery of therapeutics.* FASEB J, 2005. **19**(14): p. 1978-85.

90. Xu, W.W., et al., *GE11 peptide-conjugated nanoliposomes to enhance the combinational therapeutic efficacy of docetaxel and siRNA in laryngeal cancers.* Int J Nanomedicine, 2017. **12**: p. 6461-6470.
91. Antony, A.C., et al., *Isolation and characterization of a folate receptor from human placenta.* J Biol Chem, 1981. **256**(18): p. 9684-92.
92. Weitman, S.D., et al., *Distribution of the folate receptor GP38 in normal and malignant cell lines and tissues.* Cancer Res, 1992. **52**(12): p. 3396-401.
93. He, D., et al., *Combinatorial Optimization of Sequence-Defined Oligo(ethanamino)amides for Folate Receptor-Targeted pDNA and siRNA Delivery.* Bioconjug Chem, 2016. **27**(3): p. 647-59.
94. Muller, K., et al., *Post-PEGylation of siRNA Lipo-oligoamino Amide Polyplexes Using Tetra-glutamylated Folic Acid as Ligand for Receptor-Targeted Delivery.* Mol Pharm, 2016. **13**(7): p. 2332-45.
95. Lächelt, U., et al., *Fine-tuning of proton sponges by precise diaminoethanes and histidines in pDNA polyplexes.* Nanomedicine, 2014. **10**(1): p. 35-44.
96. Liu, L., et al., *Efficient and Tumor Targeted siRNA Delivery by Polyethylenimine-graft-polycaprolactone-block-poly(ethylene glycol)-folate (PEI-PCL-PEG-Fol).* Mol Pharm, 2016. **13**(1): p. 134-43.
97. Mislick, K.A., et al., *Transfection of folate-polylysine DNA complexes: evidence for lysosomal delivery.* Bioconjug Chem, 1995. **6**(5): p. 512-5.
98. Leamon, C.P., D. Weigl, and R.W. Hendren, *Folate copolymer-mediated transfection of cultured cells.* Bioconjug Chem, 1999. **10**(6): p. 947-57.
99. Wang, M., et al., *Engineering multifunctional bioactive citric acid-based nanovectors for intrinsical targeted tumor imaging and specific siRNA gene delivery in vitro/in vivo.* Biomaterials, 2019. **199**: p. 10-21.
100. Lee, D.J., et al., *Tumoral gene silencing by receptor-targeted combinatorial siRNA polyplexes.* J Control Release, 2016. **244**(Pt B): p. 280-291.
101. Dohmen, C., et al., *Nanosized multifunctional polyplexes for receptor-mediated siRNA delivery.* ACS Nano, 2012. **6**(6): p. 5198-208.
102. Kos, P., et al., *Dual-targeted polyplexes based on sequence-defined peptide-PEG-oligoamino amides.* J Pharm Sci, 2015. **104**(2): p. 464-75.
103. Kim, T., et al., *Dual-targeting RNA nanoparticles for efficient delivery of polymeric siRNA to cancer cells.* Chem Commun (Camb), 2020. **56**(49): p. 6624-6627.
104. Canton, I. and G. Battaglia, *Endocytosis at the nanoscale.* Chem Soc Rev, 2012. **41**(7): p. 2718-39.
105. Smith, S.A., et al., *The Endosomal Escape of Nanoparticles: Toward More Efficient Cellular Delivery.* Bioconjug Chem, 2019. **30**(2): p. 263-272.
106. Poteryaev, D., et al., *Identification of the switch in early-to-late endosome transition.* Cell, 2010. **141**(3): p. 497-508.
107. Such, G.K., et al., *Interfacing materials science and biology for drug carrier design.* Adv Mater, 2015. **27**(14): p. 2278-97.
108. Mout, R., et al., *General Strategy for Direct Cytosolic Protein Delivery via Protein-Nanoparticle Co-engineering.* ACS Nano, 2017. **11**(6): p. 6416-6421.
109. Behr, J.-P., *The proton sponge: A trick to enter cells the viruses did not exploit.* Chimia, 1997. **51**(1-2): p. 34-36.

110. Boussif, O., et al., *A versatile vector for gene and oligonucleotide transfer into cells in culture and in vivo: polyethylenimine.* Proc Natl Acad Sci U S A, 1995. **92**(16): p. 7297-301.
111. Grandinetti, G., N.P. Ingle, and T.M. Reineke, *Interaction of poly(ethylenimine)-DNA polyplexes with mitochondria: implications for a mechanism of cytotoxicity.* Mol Pharm, 2011. **8**(5): p. 1709-19.
112. Moghimi, S.M., et al., *A two-stage poly(ethylenimine)-mediated cytotoxicity: implications for gene transfer/therapy.* Mol Ther, 2005. **11**(6): p. 990-5.
113. Hu, Y., et al., *Cytosolic delivery of membrane-impermeable molecules in dendritic cells using pH-responsive core-shell nanoparticles.* Nano Lett, 2007. **7**(10): p. 3056-64.
114. Miyata, K., et al., *Polyplexes from poly(aspartamide) bearing 1,2-diaminoethane side chains induce pH-selective, endosomal membrane destabilization with amplified transfection and negligible cytotoxicity.* J Am Chem Soc, 2008. **130**(48): p. 16287-94.
115. Su, X., et al., *Synergistic antitumor activity from two-stage delivery of targeted toxins and endosome-disrupting nanoparticles.* Biomacromolecules, 2013. **14**(4): p. 1093-102.
116. von Gersdorff, K., et al., *The internalization route resulting in successful gene expression depends on both cell line and polyethylenimine polyplex type.* Mol Ther, 2006. **14**(5): p. 745-53.
117. Rejman, J., A. Bragonzi, and M. Conese, *Role of clathrin- and caveolae-mediated endocytosis in gene transfer mediated by lipo- and polyplexes.* Mol Ther, 2005. **12**(3): p. 468-74.
118. Tamura, A., M. Oishi, and Y. Nagasaki, *Enhanced cytoplasmic delivery of siRNA using a stabilized polyion complex based on PEGylated nanogels with a cross-linked polyamine structure.* Biomacromolecules, 2009. **10**(7): p. 1818-27.
119. Monnery, B.D., *Polycation-Mediated Transfection: Mechanisms of Internalization and Intracellular Trafficking.* Biomacromolecules, 2021. **22**(10): p. 4060-4083.
120. Pack, D.W., et al., *Design and development of polymers for gene delivery.* Nat Rev Drug Discov, 2005. **4**(7): p. 581-93.
121. Brunner, S., et al., *Overcoming the nuclear barrier: cell cycle independent nonviral gene transfer with linear polyethylenimine or electroporation.* Mol Ther, 2002. **5**(1): p. 80-6.
122. Hu, Q., et al., *Intracellular pathways and nuclear localization signal peptide-mediated gene transfection by cationic polymeric nanovectors.* Biomaterials, 2012. **33**(4): p. 1135-45.
123. Sutherland, R., et al., *Ubiquitous cell-surface glycoprotein on tumor cells is proliferation-associated receptor for transferrin.* Proc Natl Acad Sci U S A, 1981. **78**(7): p. 4515-9.
124. Shindelman, J.E., A.E. Ortmeyer, and H.H. Sussman, *Demonstration of the transferrin receptor in human breast cancer tissue. Potential marker for identifying dividing cells.* Int J Cancer, 1981. **27**(3): p. 329-34.
125. Collawn, J.F., et al., *Transferrin receptor internalization sequence YXRF implicates a tight turn as the structural recognition motif for endocytosis.* Cell, 1990. **63**(5): p. 1061-72.

126. Luck, A.N. and A.B. Mason, *Transferrin-mediated cellular iron delivery.* Curr Top Membr, 2012. **69**: p. 3-35.
127. Parkkinen, J., et al., *Function and therapeutic development of apotransferrin.* Vox Sang, 2002. **83 Suppl 1**: p. 321-6.
128. Kawabata, H., *Transferrin and transferrin receptors update.* Free Radic Biol Med, 2019. **133**: p. 46-54.
129. Lee, J.H., et al., *Receptor mediated uptake of peptides that bind the human transferrin receptor.* Eur J Biochem, 2001. **268**(7): p. 2004-12.
130. Prades, R., et al., *Applying the retro-enantio approach to obtain a peptide capable of overcoming the blood-brain barrier.* Angew Chem Int Ed Engl, 2015. **54**(13): p. 3967-72.
131. Stingl, G., et al., *Phase I study to the immunotherapy of metastatic malignant melanoma by a cancer vaccine consisting of autologous cancer cells transfected with the human IL-2 gene.* Hum Gene Ther, 1996. **7**(4): p. 551-63.
132. Schreiber, S., et al., *Immunotherapy of metastatic malignant melanoma by a vaccine consisting of autologous interleukin 2-transfected cancer cells: outcome of a phase I study.* Hum Gene Ther, 1999. **10**(6): p. 983-93.
133. Sasaki, K., et al., *An artificial virus-like nano carrier system: enhanced endosomal escape of nanoparticles via synergistic action of pH-sensitive fusogenic peptide derivatives.* Anal Bioanal Chem, 2008. **391**(8): p. 2717-27.
134. Davis, M.E., et al., *Evidence of RNAi in humans from systemically administered siRNA via targeted nanoparticles.* Nature, 2010. **464**(7291): p. 1067-70.
135. Wagner, E., et al., *Transferrin-polycation conjugates as carriers for DNA uptake into cells.* Proc Natl Acad Sci U S A, 1990. **87**(9): p. 3410-4.
136. Kircheis, R., et al., *Coupling of cell-binding ligands to polyethylenimine for targeted gene delivery.* Gene Ther, 1997. **4**(5): p. 409-18.
137. Kircheis, R., et al., *Polycation-based DNA complexes for tumor-targeted gene delivery in vivo.* J Gene Med, 1999. **1**(2): p. 111-20.
138. Kircheis, R., et al., *Polyethylenimine/DNA complexes shielded by transferrin target gene expression to tumors after systemic application.* Gene Ther, 2001. **8**(1): p. 28-40.
139. Kircheis, R., et al., *Tumor-targeted gene delivery of tumor necrosis factor-alpha induces tumor necrosis and tumor regression without systemic toxicity.* Cancer Gene Ther, 2002. **9**(8): p. 673-80.
140. Schaffert, D., et al., *Solid-phase synthesis of sequence-defined T-, i-, and U-shape polymers for pDNA and siRNA delivery.* Angew Chem Int Ed Engl, 2011. **50**(38): p. 8986-9.
141. Schaffert, D., N. Badgujar, and E. Wagner, *Novel Fmoc-polyamino acids for solid-phase synthesis of defined polyamidoamines.* Org Lett, 2011. **13**(7): p. 1586-9.
142. Zhang, W., et al., *Combination of sequence-defined oligoaminoamides with transferrin-polycation conjugates for receptor-targeted gene delivery.* J Gene Med, 2015. **17**(8-9): p. 161-72.
143. Zhang, W., et al., *Targeted siRNA Delivery Using a Lipo-Oligoaminoamide Nanocore with an Influenza Peptide and Transferrin Shell.* Adv Healthc Mater, 2016. **5**(12): p. 1493-504.

144. Schoenmaker, L., et al., *mRNA-lipid nanoparticle COVID-19 vaccines: Structure and stability.* Int J Pharm, 2021. **601**: p. 120586.
145. Sahin, U., et al., *BNT162b2 vaccine induces neutralizing antibodies and poly-specific T cells in humans.* Nature, 2021. **595**(7868): p. 572-577.
146. Baden, L.R., et al., *Efficacy and Safety of the mRNA-1273 SARS-CoV-2 Vaccine.* N Engl J Med, 2021. **384**(5): p. 403-416.
147. Grabbe, S., et al., *Translating nanoparticulate-personalized cancer vaccines into clinical applications: case study with RNA-lipoplexes for the treatment of melanoma.* Nanomedicine (Lond), 2016. **11**(20): p. 2723-2734.
148. Zhang, H., et al., *Delivery of mRNA vaccine with a lipid-like material potentiates antitumor efficacy through Toll-like receptor 4 signaling.* Proc Natl Acad Sci U S A, 2021. **118**(6).
149. Kranz, L.M., et al., *Systemic RNA delivery to dendritic cells exploits antiviral defence for cancer immunotherapy.* Nature, 2016. **534**(7607): p. 396-401.
150. Diken, M., et al., *mRNA: A Versatile Molecule for Cancer Vaccines.* Curr Issues Mol Biol, 2017. **22**: p. 113-128.
151. Li, Y., et al., *Single-step microfluidic synthesis of transferrin-conjugated lipid nanoparticles for siRNA delivery.* Nanomedicine, 2017. **13**(2): p. 371-381.
152. Zheng, B., et al., *Delivery of Antisense Oligonucleotide LOR-2501 Using Transferrin-conjugated Polyethylenimine-based Lipid Nanoparticle.* Anticancer Res, 2019. **39**(4): p. 1785-1793.
153. Schaffert, D., et al., *Poly(I:C)-mediated tumor growth suppression in EGF-receptor overexpressing tumors using EGF-polyethylene glycol-linear polyethylenimine as carrier.* Pharm Res, 2011. **28**(4): p. 731-41.
154. Berger, S., et al., *Correction to "Optimizing pDNA Lipo-polyplexes: A Balancing Act between Stability and Cargo Release".* Biomacromolecules, 2021. **22**(12): p. 5401.
155. Luo, J., et al., *Hyaluronate siRNA nanoparticles with positive charge display rapid attachment to tumor endothelium and penetration into tumors.* J Control Release, 2021. **329**: p. 919-933.
156. Benli-Hoppe, T., et al., *Transferrin Receptor Targeted Polyplexes Completely Comprised of Sequence-Defined Components.* Macromol Rapid Commun, 2021: p. e2100602.
157. Scholz, C. and E. Wagner, *Therapeutic plasmid DNA versus siRNA delivery: common and different tasks for synthetic carriers.* J Control Release, 2012. **161**(2): p. 554-65.
158. Wang, Y., et al., *Double Click-Functionalized siRNA Polyplexes for Gene Silencing in Epidermal Growth Factor Receptor-Positive Tumor Cells.* ACS Biomater Sci Eng, 2020. **6**(2): p. 1074-1089.
159. Klein, P.M., et al., *Folate receptor-directed orthogonal click-functionalization of siRNA lipopolyplexes for tumor cell killing in vivo.* Biomaterials, 2018. **178**: p. 630-642.
160. Truebenbach, I., et al., *Combination Chemotherapy of L1210 Tumors in Mice with Pretubulysin and Methotrexate Lipo-Oligomer Nanoparticles.* Mol Pharm, 2019. **16**(6): p. 2405-2417.
161. Jewett, J.C. and C.R. Bertozzi, *Cu-free click cycloaddition reactions in chemical biology.* Chem Soc Rev, 2010. **39**(4): p. 1272-9.

162. Tao, Y., et al., *Modular synthesis of amphiphilic chitosan derivatives based on copper-free click reaction for drug delivery.* Int J Pharm, 2021. **605**: p. 120798.
163. Debets, M.F., et al., *Aza-dibenzocyclooctynes for fast and efficient enzyme PEGylation via copper-free (3+2) cycloaddition.* Chem Commun (Camb), 2010. **46**(1): p. 97-9.
164. Agard, N.J., et al., *A comparative study of bioorthogonal reactions with azides.* ACS Chem Biol, 2006. **1**(10): p. 644-8.
165. Plank, C., et al., *Gene transfer into hepatocytes using asialoglycoprotein receptor mediated endocytosis of DNA complexed with an artificial tetra-antennary galactose ligand.* Bioconjug Chem, 1992. **3**(6): p. 533-9.
166. Naldini, L., *Gene therapy returns to centre stage.* Nature, 2015. **526**(7573): p. 351-60.
167. Samaridou, E., J. Heyes, and P. Lutwyche, *Lipid nanoparticles for nucleic acid delivery: Current perspectives.* Adv Drug Deliv Rev, 2020. **154-155**: p. 37-63.
168. Kulkarni, J.A., et al., *The current landscape of nucleic acid therapeutics.* Nat Nanotechnol, 2021. **16**(6): p. 630-643.
169. Vighi, E., et al., *pDNA condensation capacity and in vitro gene delivery properties of cationic solid lipid nanoparticles.* Int J Pharm, 2010. **389**(1-2): p. 254-61.
170. Pilkington, E.H., et al., *From influenza to COVID-19: Lipid nanoparticle mRNA vaccines at the frontiers of infectious diseases.* Acta Biomater, 2021. **131**: p. 16-40.
171. Templeton, N.S., et al., *Improved DNA: liposome complexes for increased systemic delivery and gene expression.* Nat Biotechnol, 1997. **15**(7): p. 647-52.
172. Cullis, P.R. and M.J. Hope, *Lipid Nanoparticle Systems for Enabling Gene Therapies.* Mol Ther, 2017. **25**(7): p. 1467-1475.
173. Patel, S., et al., *Author Correction: Naturally-occurring cholesterol analogues in lipid nanoparticles induce polymorphic shape and enhance intracellular delivery of mRNA.* Nat Commun, 2020. **11**(1): p. 3435.
174. Akinc, A., et al., *Development of lipidoid-siRNA formulations for systemic delivery to the liver.* Mol Ther, 2009. **17**(5): p. 872-9.
175. Zhu, X., et al., *Surface De-PEGylation Controls Nanoparticle-Mediated siRNA Delivery In Vitro and In Vivo.* Theranostics, 2017. **7**(7): p. 1990-2002.
176. Che, J., et al., *DSPE-PEG: a distinctive component in drug delivery system.* Curr Pharm Des, 2015. **21**(12): p. 1598-605.
177. Zhang, Z. and J. Yao, *Preparation of irinotecan-loaded folate-targeted liposome for tumor targeting delivery and its antitumor activity.* AAPS PharmSciTech, 2012. **13**(3): p. 802-10.
178. Kim, J., et al., *Self-assembled mRNA vaccines.* Adv Drug Deliv Rev, 2021. **170**: p. 83-112.
179. Ryals, R.C., et al., *The effects of PEGylation on LNP based mRNA delivery to the eye.* PLoS One, 2020. **15**(10): p. e0241006.
180. Knop, K., et al., *Poly(ethylene glycol) in drug delivery: pros and cons as well as potential alternatives.* Angew Chem Int Ed Engl, 2010. **49**(36): p. 6288-308.

181. Dammes, N., et al., *Conformation-sensitive targeting of lipid nanoparticles for RNA therapeutics.* Nat Nanotechnol, 2021. **16**(9): p. 1030-1038.
182. Patel, S., et al., *Lipid nanoparticles for delivery of messenger RNA to the back of the eye.* J Control Release, 2019. **303**: p. 91-100.
183. Krzyszton, R., et al., *Microfluidic self-assembly of folate-targeted monomolecular siRNA-lipid nanoparticles.* Nanoscale, 2017. **9**(22): p. 7442-7453.
184. Adams, D., et al., *Patisiran, an RNAi Therapeutic, for Hereditary Transthyretin Amyloidosis.* N Engl J Med, 2018. **379**(1): p. 11-21.
185. Zhang, M.M., et al., *The growth of siRNA-based therapeutics: Updated clinical studies.* Biochem Pharmacol, 2021. **189**: p. 114432.
186. Debacker, A.J., et al., *Delivery of Oligonucleotides to the Liver with GalNAc: From Research to Registered Therapeutic Drug.* Mol Ther, 2020. **28**(8): p. 1759-1771.
187. Jayaraman, M., et al., *Maximizing the potency of siRNA lipid nanoparticles for hepatic gene silencing in vivo.* Angew Chem Int Ed Engl, 2012. **51**(34): p. 8529-33.
188. Ramishetti, S., et al., *A Combinatorial Library of Lipid Nanoparticles for RNA Delivery to Leukocytes.* Adv Mater, 2020. **32**(12): p. e1906128.
189. Algarni, A., et al., *In vivo delivery of plasmid DNA by lipid nanoparticles: the influence of ionizable cationic lipids on organ-selective gene expression.* Biomater Sci, 2022.
190. Olbrich, C., et al., *Cationic solid-lipid nanoparticles can efficiently bind and transfect plasmid DNA.* J Control Release, 2001. **77**(3): p. 345-55.
191. Penacho, N., et al., *Transferrin-associated lipoplexes as gene delivery systems: relevance of mode of preparation and biophysical properties.* J Membr Biol, 2008. **221**(3): p. 141-52.

7. Publications

Benli-Hoppe T,[+] **Göl Öztürk Ş**,[+] Öztürk Ö, Berger S, Wagner E, Yazdi M. Transferrin Receptor Targeted Polyplexes Completely Comprised of Sequence-Defined Components, *Macromol Rapid Commun*. 2021 Oct 29:e2100602.

[+] Equally contributing first authors

8. Acknowledgements

Words cannot express my feelings! During the past four years, I would like to thank all the people that either directly by collaborating in the lab or indirectly by supporting in my personal life.

First and foremost, I would like to thank my supervisor Prof. Dr. Ernst Wagner for giving me the opportunity to do my Ph.D. in his research group. I am deeply grateful for his scientific support and professional guidance. I have learned a lot under his supervision. I will continue to follow his footsteps and teachings at my future scientific carrier.

I would like to thank YLSY fellowships granted by Turkish Ministry of Education as support to my Ph.D. studies at Ludwig-Maximilians-Universität Munich. I want to special thank General Consul of Turkish Republic Mehmet Günay and Education Attaché Prof. Dr. Mustafa Çakır for their support and guidance.

I am also grateful to all my colleagues for their collaborations without whom this thesis would not be possible. Special thanks to Teoman Benli-Hoppe, Mina Yazdi and Simone Berger whom I worked together in reTfR project. I would like to thank Franziska Haase and Lun Peng for their collaboration at LNP project. I also want to thank Dr. Ana Krhac Levacic and Dr. Wei Zhang for teaching me the all experiments and sharing their knowledge at the beginning of my Ph.D. I would like to thank Özgür Öztürk for his TEM measurement and Miriam Höhn for instruction of the FCS and cell culture. I am very grateful to Wolfgang Rödl for repairing any computer or equipment; Melinda Kiss and Markus Kovac for keeping the everyday life in the lab running and Olga Brück for her organization

skills. I thank Yi Lin and Janin Germer for their discussions at the Cas9 task force. Many thanks to Prof. Dr. Ulrich Lächelt for valuable discussions and chocolates in every December until he left. I want to thank all other members of the Wagner group for the nice working atmosphere in the lab.

Also, I thank all my friends. Thank you so much Hande, Elvan, Pelin and Gizem for your perfect friendship and your great advice whenever I need. I would like to thank my YLSY friends Merve, Selin, Elif, Mahmut, Kaan, Melis and Mehmet who I met in Munich and had fun together.

Last but not least, my deepest thanks to my whole family. I am deeply grateful to my parents Nezahat and Hüseyin for their support and trust during whole my life. I am happy to being their daughter. You are my biggest chance in this life. Thank you my brothers Furkan and Cabir for making my life so enjoyable. Thank you Özgür for his patience, for listening to my worries, for encouraging me and always believing in me.

Teşekkürler!